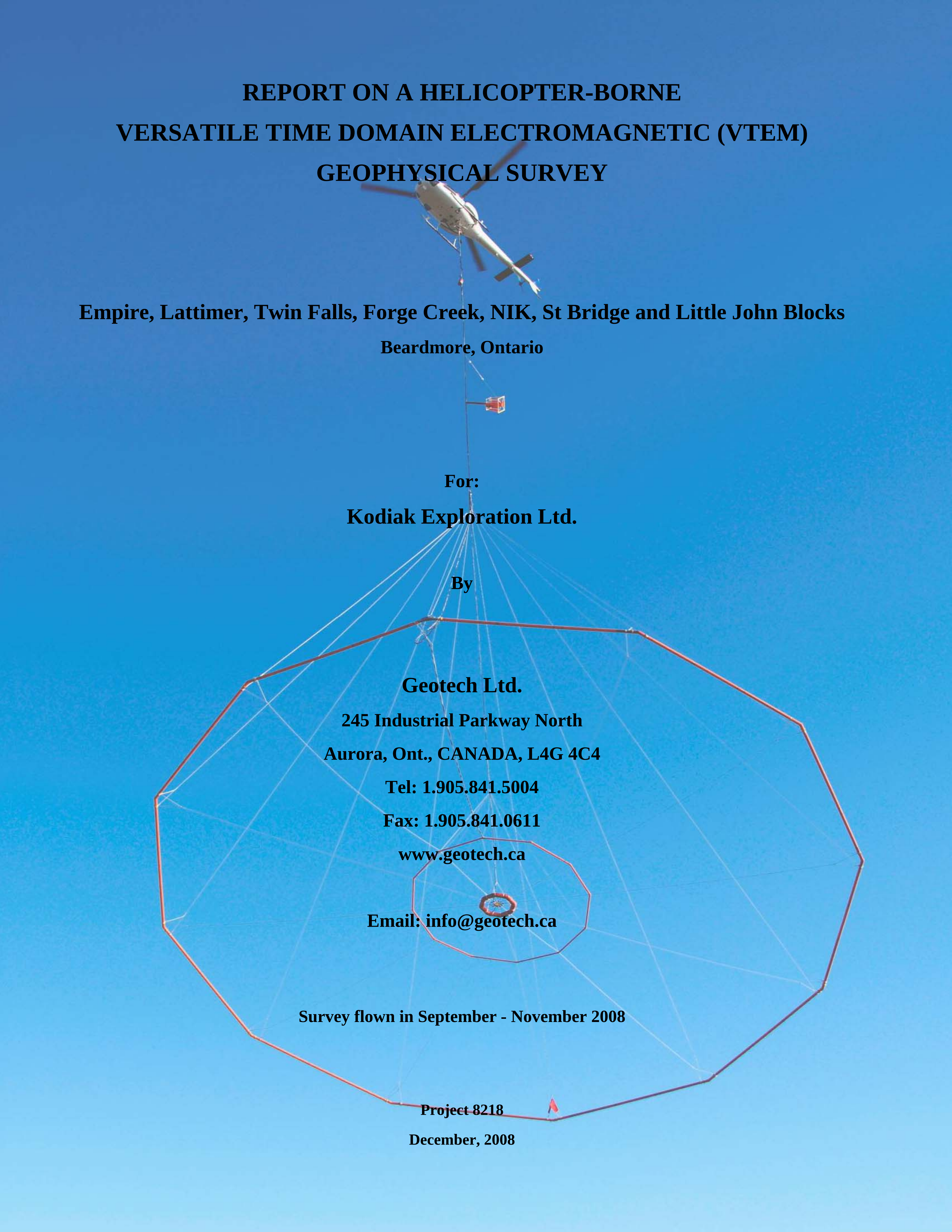

REPORT ON A HELICOPTER-BORNE VERSATILE TIME DOMAIN ELECTROMAGNETIC (VTEM) GEOPHYSICAL SURVEY

Empire, Lattimer, Twin Falls, Forge Creek, NIK, St Bridge and Little John Blocks

Beardmore, Ontario

For:

Kodiak Exploration Ltd.

By

Geotech Ltd.

245 Industrial Parkway North

Aurora, Ont., CANADA, L4G 4C4

Tel: 1.905.841.5004

Fax: 1.905.841.0611

www.geotech.ca

Email: info@geotech.ca

Survey flown in September - November 2008

Project 8218

December, 2008

TABLE OF CONTENTS

Executive Summary **4**
1. INTRODUCTION **5**
1.1 General Considerations 5
1.2 Survey Location and Specifications 6
1.3 Topographic Relief and Cultural Features 6
2. DATA ACQUISITION **7**
2.1 Survey Area 7
2.2 Survey Operations 8
2.3 Flight Specifications 10
2.4 Aircraft and Equipment 10
2.4.1 Survey Aircraft 10
2.4.2 Electromagnetic System 10
2.4.3 Airborne magnetometer 14
2.4.4 Radar Altimeter 14
2.4.5 GPS Navigation System 14
2.4.6 Digital Acquisition System 14
2.4.7 Base Station 15
3. PERSONNEL **16**
4. DATA PROCESSING AND PRESENTATION **17**
4.1 Flight Path 17
4.2 Electromagnetic Data 17
4.3 Anomaly Section 18
4.4 Magnetic Data 19
5. DELIVERABLES **20**
5.1 Survey Report 20
5.2 Maps 20
5.3 Digital Data 20
6. PRELIMINARY INTERPRETATION **24**
6.1 Geological Context and Mineralization 24
6.2 Possible Principles of Interpretation and analysis of the geophysical data 25
7. CONCLUSIONS AND RECOMMENDATIONS **27**
7.1 Conclusions 27
7.2 Recommendations 27

APPENDICES

A. Survey location map 28
B. Survey Block Coordinates 38
C. VTEM Waveform 39
D. Geophysical Maps 40
E. Modelling VTEM Data 53
F. EM Time Constant (TAU) Analysis 64
G. Electromagnetic Anomaly Listing 69

LIST OF TABLES

Table 1 - Survey block 7
Table 2 - Survey schedule 8
Table 3 - Decay Sampling Scheme 12
Table 4 - Acquisition Sampling Rates 14
Table 5 - Geosoft GDB Data Format 21

LIST OF FIGURES

Figure 1 - Property Location 5
Figure 2 - Google Image with Flight Path 6
Figure 3 - VTEM Configuration 11
Figure 4 - VTEM Waveform & Sample Times 11
Figure 5 - Conventional VTEM system configuration 13
Figure 6 - EM Anomaly Symbols 18
Figure 7 - EM response from subvertical thin plate target (Lattimer block) 25
Figure 8 - Axes of conductive subvertical zones with CVG grid. Lattimer-Solo-Maki block. 25
Figure 9 - Axes of conductive zones (blue lines) and linear features of magnetic field (red lines). Lattimer-Solo-Maki block. 26
Figure 10 - Results of the modeling of EM anomaly on 7910 line of east part of Lattimer block. 26

REPORT ON A HELICOPTER-BORNE VERSATILE TIME DOMAIN ELECTROMAGNETIC SURVEY

Empire, Lattimer, Forge Creek, Twin Falls, NIK, St Bridge and Little John Blocks
Beardmore, Ontario

Executive Summary

During September 18th to November 3rd, 2008 Geotech Ltd. carried out a helicopter-borne geophysical survey for Kodiak Exploration Ltd over Empire, Lattimer, Forge Creek, Twin Falls, NIK, St Bridge and Little John blocks near Beardmore, Ontario, Canada.

Principal geophysical sensors included a versatile time domain electromagnetic (VTEM) system and a caesium magnetometer. Ancillary equipment included a GPS navigation system and a radar altimeter. A total of 4964 line-km were flown.

The survey operations were based in Geraldton, Ontario. In-field data quality assurance and preliminary processing were carried out on a daily basis during the acquisition phase. Preliminary and final data processing, including generation of digital data and map products, were undertaken from the office of Geotech Ltd. in Aurora, Ontario.

The processed survey results are presented as stacked profiles for the electromagnetics and the following grid contours:

- Total magnetic intensity
- B-field time gate 1.953 ms
- Calculated Time Constant (TAU)B-field and dB/dt
- Calculated Vertical Derivative

Digital data includes all electromagnetic and magnetic products, plus ancillary data including the waveform.

This report describes the logistics of the survey acquisition phase and the final data processing phase. The geophysical results are briefly discussed and interpreted using EM anomaly picking and time constant (Tau) analysis, as well as magnetic derivative analysis.

1. INTRODUCTION

1.1 General Considerations

These services are the result of the Agreement made between Geotech Ltd. and Kodiak Exploration Ltd to perform a helicopter-borne geophysical survey over the 7 blocks, located near the town of Beardmore in northern Ontario, Canada (Figure 1).

Bahman Bayat acted on behalf of Kodiak Exploration Ltd during the data acquisition and data processing phases of this project.

The geophysical surveys consisted of heliborne EM using the versatile time-domain electromagnetic (VTEM) system and aeromagnetics using a caesium magnetometer. A total of 4964 line-km of geophysical data were acquired during the survey. The survey area is shown in Figure 2.

The crew was based at the Roxy Place in the town of Beardmore, Ontario for the acquisition phase of the survey, as shown in Section 2 of this report. Survey flying started on September 18th and was completed on November 3rd, 2008

In-field data quality control and quality assurance as well as preliminary data processing were carried out daily during the acquisition phase of the project. Final data processing followed immediately after the end of the survey. Final reporting, data presentation and archiving were completed from the Aurora office of Geotech Ltd. in December, 2008.

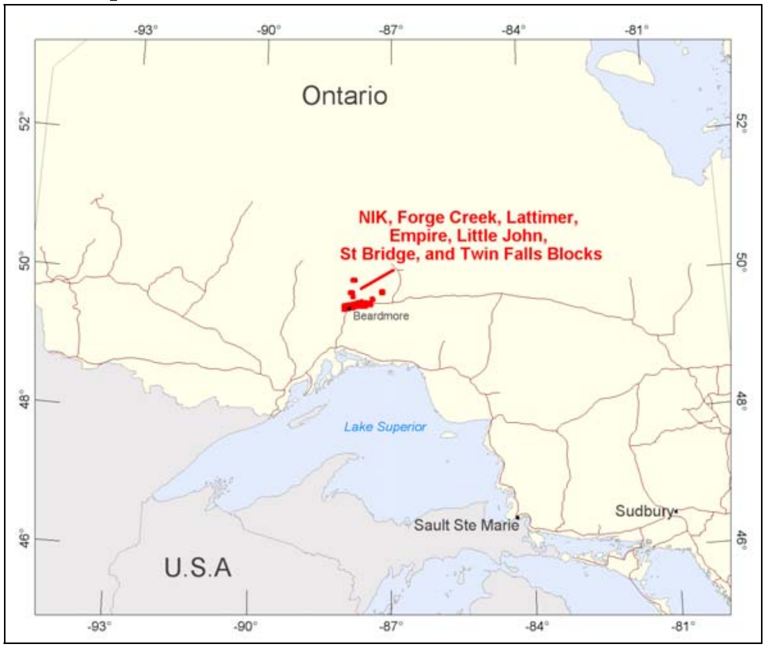

Figure 1 - Property Location

1.2 Survey Location and Specifications

The Empire block is located directly over the town of Beardmore, ON while the other blocks are all located to the east and north of Beardmore. The blocks were flown at 100 metre traverse line spacing wherever possible with flight directions of N 0° E, while the tie lines were flown perpendicular to the traverse lines at a spacing of 1000 meters with flight directions of N 90° E. For more detailed information on the flight spacing and direction see Table 1.

1.3 Topographic Relief and Cultural Features

Topographically, this area exhibits a moderate relief, with an elevation ranging from 263-486 metres above sea level (Figure 2). Special care is recommended in identifying any potential cultural features from other sources that might be recorded in the data. These survey blocks are covered by NTS (National Topographic Survey) of Canada sheets 042L04, 042E11, 042E12, 042E13, 042E14 and 052H09.

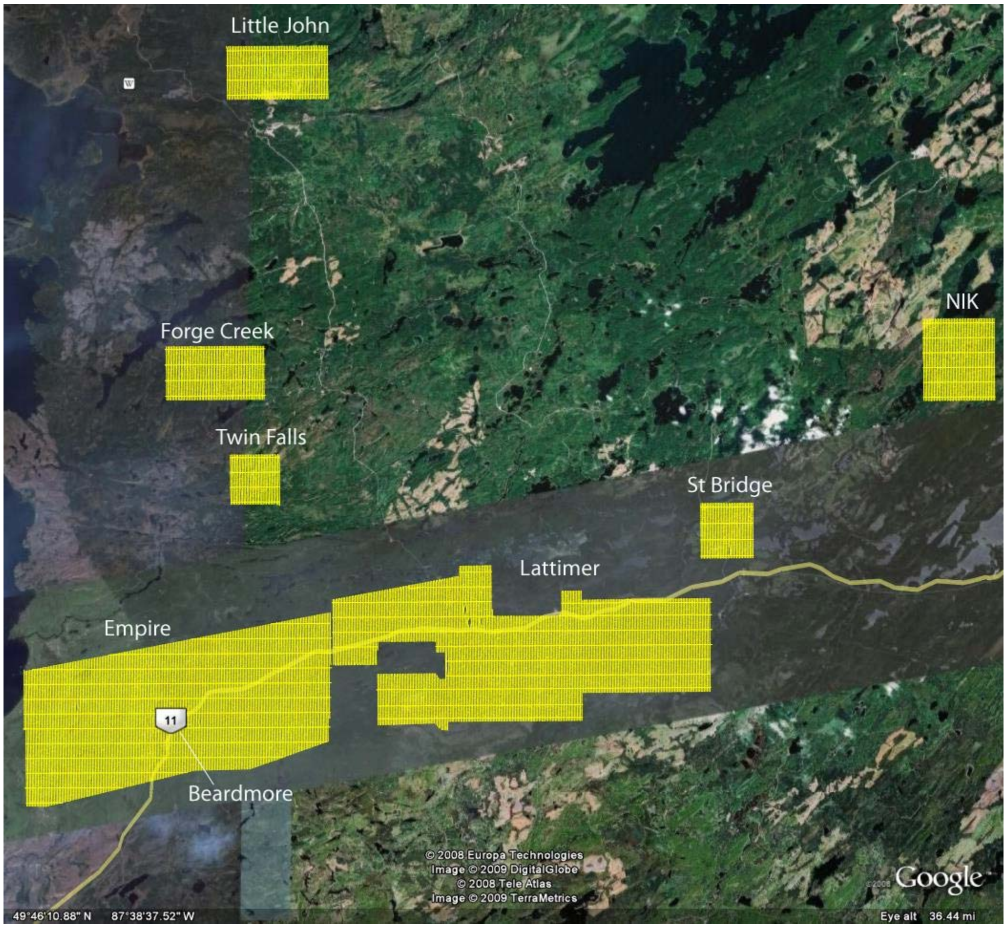

Figure 2 - Google Image with Flight Path

2. DATA ACQUISITION

2.1 Survey Area

The block (see Figure 2 and Location map in Appendix A) and general flight specifications are as follows:

Table 1 - Survey block

Survey block	Line spacing (m)	Area (km^2)	Planned Line-km	Actual Line-km[1]	Flight direction	Line number
Twin Falls	100	11.5	107.5	114	N 0° E / N 180° E	L5000-L5330
	Tie:1000		13.4	13.4	N 90° E / N 270° E	T5500-T5530
NIK	100	27.5	252.8	271	N 0° E / N 180° E	L3000-L3480
	Tie:1000		29.1	29.4	N 90° E / N 270° E	T3800-T3850
Forge Creek	100	24.7	229.6	243	N 0° E / N 180° E	L2000-L2660
	Tie:1000		26.5	27	N 90° E / N 270° E	T2800-T2830
Little John	100	25.5	221.5	249	N 0° E / N 180° E	L1000-L1680
	Tie:1000		27.3	27.5	N 90° E / N 270° E	T1800-T1830
Empire	100	193	1860.7	1904	N 0° E / N 180° E	L9970-L12050
	Tie:1000		186.8	190.5	N 90° E / N 270° E	T12610-T12490
Lattimer[2]	100	190	1688.2	2230	N 0° E / N 180° E	L6010-L8560
	Tie:1000		182	235.2	N 90° E / N 270° E	T8910-T9000
St Bridge	100	13.7	124.6	134	N 0° E / N 180° E	L4000-L4350
	Tie:1000		14	14.4	N 90° E / N 270° E	T4500-T4530
TOTAL		485.9	4964	5682.4		

Survey block boundaries coordinates are provided in Appendix B.

[1] Note: Actual line-km represents the total line-km contained in the final databases. These line-km normally exceed the Planned line-km, as indicated in the survey NAV files
2 Note: Actual line-km has been merged with the blocks of Maki and Solomon Pillar from project 8181.

2.2 Survey Operations

Survey operations were based out of the Roxy Place near Beardmore, ON from September 18th to November 3rd 2008. The following table shows the timing of the flying.

Table 2 - Survey schedule

Date	Flight #	Flown KM	Block	Crew location	Comments
09-18-2008				Beardmore, ON	Arrived Geraldton and set up base
09-19-2008	1-3	282	Nik	Beardmore	Production
09-20-2008	4-6	167	Nik	Beardmore	Production
09-21-2008	7-9	304	Lattimer	Beardmore	Production
09-22-2008	10-12	327	Lattimer	Beardmore	Production
09-23-2008	13-14	132	St.Bridge	Beardmore	Limited production-fog and gusty winds
09-24-2008				Beardmore	No production-fog, low ceiling and strong winds
09-25-2008	15-17	397	Lattimer	Beardmore	Production
09-26-2008				Beardmore	No production-low ceiling and thunder showers
09-27-2008				Beardmore	No production-low ceiling and rain
09-28-2008	18-20	186	Lattimer	Beardmore	Limited production-fog
09-29-2008				Beardmore	No production-low ceiling and rain
09-30-2008				Beardmore	No production-low ceiling and rain
10-01-2008				Beardmore	No production-rain
10-02-2008				Beardmore	No production-low ceiling and snow
10-03-2008				Beardmore	No production-low ceiling and snow
10-04-2008	21-22	257	Lattimer	Beardmore	Production
10-05-2008				Beardmore	No production-bird damaged
10-06-2008				Beardmore	Crew fixing the bird
10-07-2008	24		Empire	Beardmore	Fixed the bird, performed test flight.
10-08-2008				Beardmore	No production-low ceiling and rain
10-09-2008				Beardmore	No production-low ceiling and rain
10-10-2008	25-27	116	Lattimer	Beardmore	Limited production-reflew some lines
10-11-2008	28	123	Lattimer, St Bridge and Twin falls	Beardmore	Limited production-rain in the morning
10-12-2008	29-30	119	Empire ,Twin Falls	Beardmore	Limited production-rain in the morning
10-13-2008	31-32	163	Twin Falls, Forge Creek	Beardmore	Production
10-14-2008				Beardmore	No production-low ceiling and rain
10-15-2008	33-34	93	Forge Creek	Beardmore	Limited production-rain and high winds
10-16-2008	35-36	134	Forge Creek, Little John and Empire	Beardmore	Limited production-low ceiling in the morning
10-17-2008	37	94	Little John	Beardmore	Limited production-helicopter problem

Date	Flight #	Flown KM	Block	Crew location	Comments
10-18-2008	38-39	122	Little John	Beardmore	Limited production-low ceiling in the morning
10-19-2008				Beardmore	No production-low ceiling and rain
10-20-2008				Beardmore	No production-system testing
10-21-2008				Beardmore	No production-system testing
10-22-2008				Beardmore	No production-system testing
10-23-2008				Beardmore	Completed system tests
10-24-2008	40-41	222	Empire, Little John	Beardmore	Production
10-25-2008				Beardmore	No production- rain
10-26-2008				Beardmore	No production-bird damaged
10-27-2008				Beardmore	No production-low ceiling and snow
10-28-2008	42	73	Empire	Beardmore	Low production-low ceiling and snow
10-29-2008	43-45	473	Empire	Beardmore	Production
10-30-2008	46-47	314	Empire	Beardmore	Production
10-31-2008	48-50	405	Empire	Beardmore	Production
11-01-2008	51-53	461	Empire	Beardmore	Production
11-02-2008				Beardmore	Reflights
11-03-2008				Beardmore	Job complete

2.3 Flight Specifications

The helicopter was maintained at a mean height of 78 meters above the ground with a nominal survey speed of 80 km/hour for the survey. This allowed for a nominal EM sensor terrain clearance was 43 meters and a magnetic sensor clearance of 65 meters. The data recording rates of the data acquisition was 0.1 second for electromagnetics and magnetometer, 0.2 second for altimeter and GPS. This translates to a geophysical reading about every 2 meters along flight track. Navigation was assisted by a GPS receiver and data acquisition system, which reports GPS co-ordinates as latitude/longitude and directs the pilot over a pre-programmed survey grid.

The operator was responsible for monitoring of the system integrity. He also maintained a detailed flight log during the survey, tracking the times of the flight as well as any unusual geophysical or topographic feature.

On return of the aircrew to the base camp the survey data was transferred from a compact flash card (PCMCIA) to the data processing computer. The data were then uploaded via ftp to the Geotech office in Aurora for daily quality assurance and quality control by qualified personnel, operating remotely.

2.4 Aircraft and Equipment

2.4.1 Survey Aircraft

The survey was flown using a Eurocopter Aerospatiale 350 B2 helicopter, registration C-GCYE. The helicopters were operated by Expedition Helicopters Ltd. Installation of the geophysical and ancillary equipment was carried out by Geotech Ltd.

2.4.2 Electromagnetic System

The electromagnetic system was a Geotech Time Domain EM (VTEM) system. The configuration is as indicated in Figure 3 below.

Receiver and transmitter coils are concentric and Z-direction oriented. The loops were towed at a mean distance of 35 meters below the aircraft as shown in Figure 5. The receiver decay recording scheme is shown diagrammatically in Figure 4.

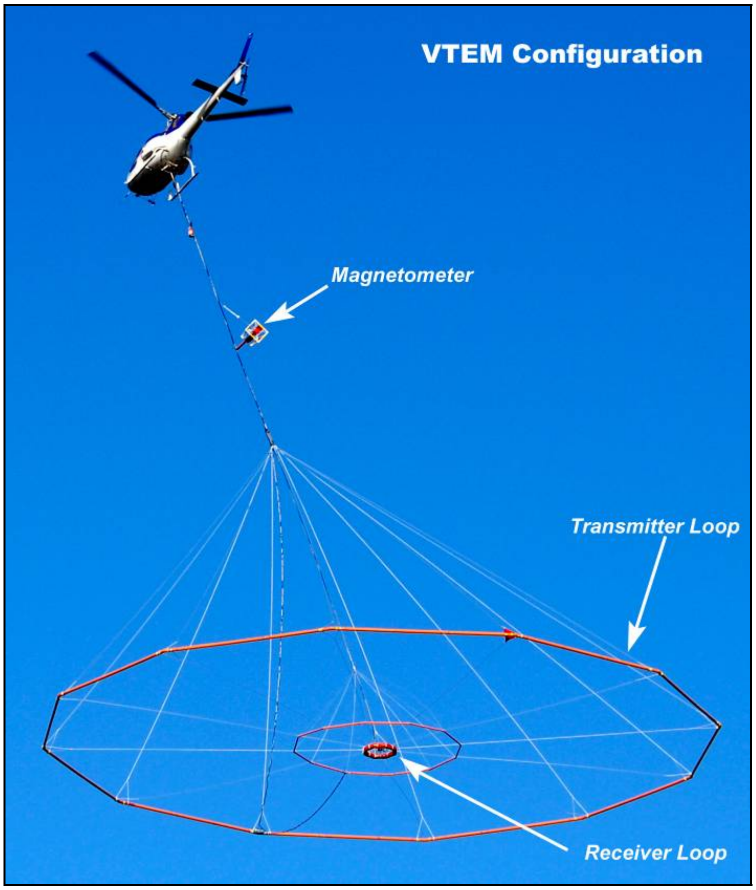

Figure 3 - VTEM Configuration

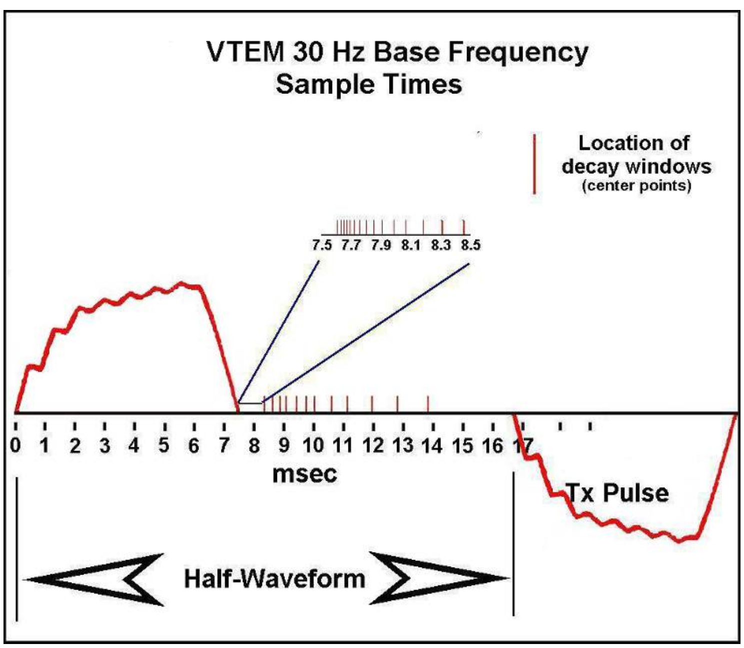

Figure 4 - VTEM Waveform & Sample Times

The complete VTEM decay sampling scheme is shown in Table 3 below. Twenty-four time measurement gates[3] (ch10 to ch33) were used for the final data processing in the range from 120 to 6578 µ sec, as shown in Table 5.

Table 3 - Decay Sampling Scheme

VTEM Decay Sampling scheme				
Array	(Microseconds)			
Index	Time Gate	Start	End	Width
0	0			
1	10	10	21	11
2	21	16	26	11
3	31	26	37	11
4	42	37	47	11
5	52	47	57	10
6	62	57	68	11
7	73	68	78	11
8	83	78	91	13
9	99	91	110	19
10	120	110	131	21
11	141	131	154	24
12	167	154	183	29
13	198	183	216	34
14	234	216	258	42
15	281	258	310	53
16	339	310	373	63
17	406	373	445	73
18	484	445	529	84
19	573	529	628	99
20	682	628	750	123
21	818	750	896	146
22	974	896	1063	167
23	1151	1063	1261	198
24	1370	1261	1506	245
25	1641	1506	1797	292
26	1953	1797	2130	333
27	2307	2130	2526	396
28	2745	2526	3016	490
29	3286	3016	3599	583
30	3911	3599	4266	667
31	4620	4266	5058	792
32	5495	5058	6037	979
33	6578	6037	7203	1167
34	7828	7203	8537	1334
35	9245	8537	10120	1584

3 Note: Measurement times-delays are referenced to time-zero marking the end of the transmitter current turn-off, as illustrated in Figure 4 and Appenix C.

VTEM system parameters:

<u>Transmitter Section</u>

- Transmitter coil diameter: 26 m
- Number of turns: 4
- Transmitter base frequency: 30 Hz
- Peak current: 175 A
- Pulse width: 7.2 ms
- Duty cycle: 43%
- Peak dipole moment: 372,000 nIA
- Nominal terrain clearance: 43 m
-

<u>Receiver Section</u>

- Receiver coil diameter: 1.2 m
- Number of turns: 100.
- Effective coil area: 113.04 m^2
- Wave form shape: trapezoid
- Power Line Monitor: 60 Hz
-

<u>Magnetometer</u>

- Nominal terrain clearance: 65 m

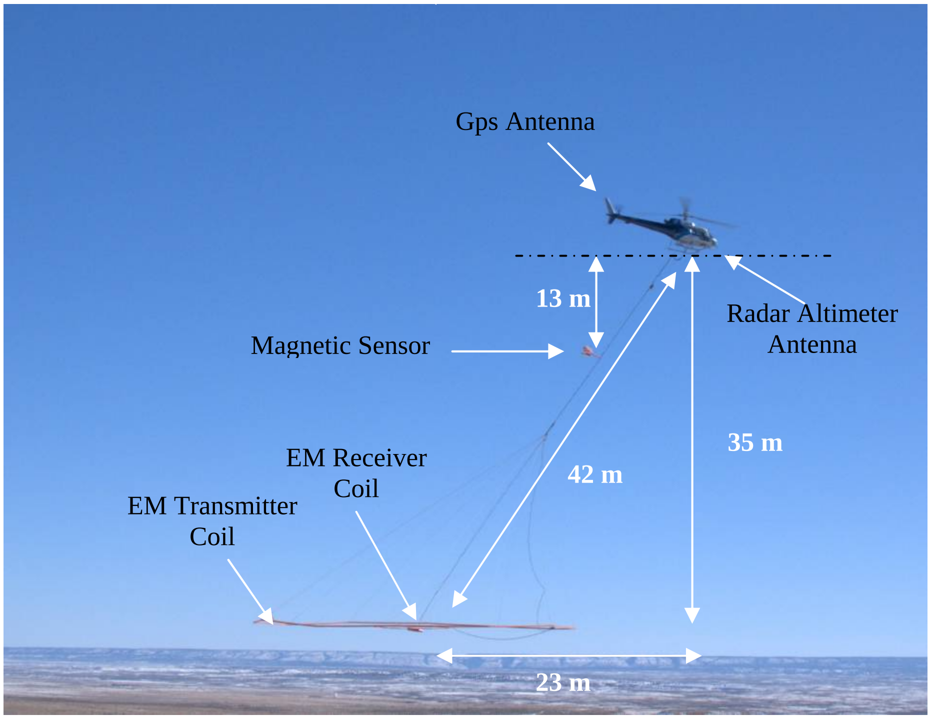

Figure 5 - Conventional VTEM system configuration

2.4.3 Airborne magnetometer

The magnetic sensor utilized for the survey was a Geometrics optically pumped caesium vapour magnetic field sensor, mounted in a separated bird, 13 metres below the helicopter, as shown in Figure 5. The sensitivity of the magnetic sensor is 0.02 nanoTesla (nT) at a sampling interval of 0.1 seconds. The magnetometer sends the measured magnetic field strength as nanoTesla to the data acquisition system via the RS-232 port.

2.4.4 Radar Altimeter

A Terra TRA 3000/TRI 40 radar altimeter was used to record terrain clearance. The antenna was mounted beneath the bubble of the helicopter cockpit (Figure 5).

2.4.5 GPS Navigation System

The navigation system used was a Geotech PC based unit consisting of a NovAtel's CDGPS (Canada-Wide Differential Global Positioning System Correction Service) enabled OEM4-G2-3151W GPS receiver, The Geotech navigate software, a full screen display with controls in front of the pilot to direct the flight and a NovAtel GPS antenna mounted on the helicopter tail (Figure 5). As many as 11 GPS and two CDGPS satellites may be monitored at any one time. The positional accuracy or circular error probability (CEP) is 1.8 m, with CDGPS active, it is 1.0 m. The co-ordinates of the block were set-up prior to the survey and the information was fed into the airborne navigation system.

2.4.6 Digital Acquisition System

A Geotech data acquisition system recorded the digital survey data on an internal compact flash card. Data is displayed on an LCD screen as traces to allow the operator to monitor the integrity of the system. The data type and sampling interval as provided in Table 4.

Table 4 - Acquisition Sampling Rates

DATA TYPE	SAMPLING
TDEM	0.1 sec
Magnetometer	0.1 sec
GPS Position	0.2 sec
Radar Altimeter	0.2 sec

2.4.7 Base Station

A combined magnetometer/GPS base station was utilized on this project. A Geometrics Caesium vapour magnetometer was used as a magnetic sensor with a sensitivity of 0.001 nT. The base station was recording the magnetic field together with the GPS time at 1 Hz on a base station computer.

The base station magnetometer sensor was installed in an isolated area in an area residents backyard (Lat 49°36'50.80"N / Long 87°56"26.54"W), away from electric transmission lines and moving ferrous objects such as motor vehicles. The base station data were backed-up to the data processing computer at the end of each survey day.

3. PERSONNEL

The following Geotech Ltd. personnel were involved in the project.

<u>Field:</u>

Project Manager:	Les Moschuk (Office)
Data QC/QA:	Nick Venter (Office) Emilio Schein
Crew chief:	Robert Amirault
Operator:	Igor Kartashov

The survey pilot and the mechanical engineer were employed directly by the helicopter operator - Expedition Helicopters Ltd.

Pilot:	Marcel Bourchard

<u>Office:</u>

Preliminary Data Processing:	Nick Venter
Final Data Processing:	Alex Prikhodko
Interpretation:	Alex Prikhodko
Final Data QC:	Neil Fiset
Reporting/Mapping:	Wendy Acorn

Data acquisition phases were carried out under the supervision of Andrei Bagrianski, P. Geo, Surveys Manager. Processing phases were carried out under the supervision of Jean Legault, P. Geo, Manager of Processing and Interpretation. The overall contract management and customer relations were by Paolo Berardelli.

4. DATA PROCESSING AND PRESENTATION

Data compilation and processing were carried out by the application of Geosoft OASIS Montaj and programs proprietary to Geotech Ltd.

4.1 Flight Path

The flight path, recorded by the acquisition program as WGS 84 latitude/longitude, was converted into the NAD83 Datum, UTM Zone 16N coordinate system in Oasis Montaj.

The flight path was drawn using linear interpolation between x, y positions from the navigation system. Positions are updated every second and expressed as UTM easting's (x) and UTM northing's (y).

4.2 Electromagnetic Data

A three stage digital filtering process was used to reject major sferic events and to reduce system noise. Local sferic activity can produce sharp, large amplitude events that cannot be removed by conventional filtering procedures. Smoothing or stacking will reduce their amplitude but leave a broader residual response that can be confused with geological phenomena. To avoid this possibility, a computer algorithm searches out and rejects the major sferic events. The filter used was a 16 point non-linear filter.

The signal to noise ratio was further improved by the application of a low pass linear digital filter. This filter has zero phase shift which prevents any lag or peak displacement from occurring, and it suppresses only variations with a wavelength less than about 1 second or 15 metres. This filter is a symmetrical 1 second linear filter.

The results are presented as stacked profiles of EM voltages for the time gates, in linear - logarithmic scale for both B-field and dB/dt response. B-field time channel recorded at 1.953 milliseconds after the termination of the impulse is also presented as colour image.

Generalized modeling results of VTEM data, written by consultant Roger Barlow and Nasreddine Bournas, P. Geo., are shown in Appendix E.

Graphical representations of the VTEM transmitter input current and the output voltage of the receiver coil are shown in Appendix C.

4.3 Anomaly Section

The EM data were subjected to an anomaly recognition process using all time domain geophysical channels and using both the B-Field and dB/dt profiles. The resulting EM anomaly picks are presented as overlays on all maps.

Each individual conductor pick is represented by an anomaly symbol classified according to calculated conductance[4] (Figure 6).The conductances were obtained directly from the EM dB/dt and B-Field time constants (Tau) [5] using the oblate spheroid conductive model (McNeil, 1980)[6]. Identified anomalies were classified into one of five categories. The anomaly symbol is accompanied by postings denoting the calculated dB/dt conductance[7], calculated dB/dt and B-field decay constant (Tau). Each symbol is also given an identification letter label, unique to each flight line. The anomaly symbol legend is given below.

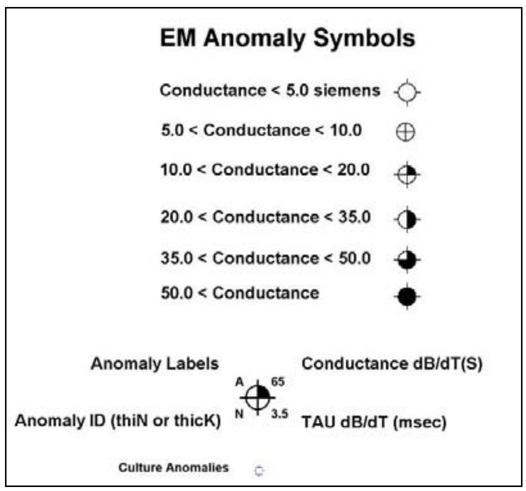

Figure 6 - EM Anomaly Symbols

EM anomaly symbols are presented in all final maps, i.e. VTEM profiles and total magnetic intensity grid. The anomalous responses have been picked on each line, reviewed and edited by an interpreter on a line by line basis to discriminate between bedrock, overburden and culture conductors. The new channels were created in each of the Geosoft "XYZ" tables for the block. The identified time domain electromagnetic VTEM anomalies are listed in Appendix G.

---

[4] Note: The conductances were obtained from the dB/dt EM time constant (Tau) whose relationship were derived using the oblate model of McNeil (1980).
[5] Note: An explanation of the EM time constant (Tau) approach to VTEM data is provided in Appendix F.
6 McNeil, J.D. (1980. Applications of transient electromagnetic techniques, Technical note TN-7, Geonic Ltd., Mississauga, ON, 17 pp.
7 Note: q/a ratio set to equal 0.0125 for VTEM dB/dt time constant of 3.65 msec and conductivity thickness (δt) equal to 73.2 siemens, over Eagle Ore Deposit, near Webequie, ON.(A. Prikhodko, Geotech, pers.comm., 12-2008)

4.4 Magnetic Data

The processing of the magnetic data involved the correction for diurnal variations by using the digitally recorded ground base station magnetic values. The base station magnetometer data were edited and merged into the Geosoft GDB database on a daily basis. The aeromagnetic data were corrected for diurnal variations by subtracting the observed magnetic base station deviations.

Tie line levelling was carried out by adjusting intersection points along traverse lines. A micro-levelling procedure was applied to remove persistent low-amplitude components of flight-line noise remaining in the data.

The corrected magnetic data were interpolated between survey lines using a random point gridding method to yield x-y grid values for a standard grid cell size of approximately 0.25 cm at the mapping scale. The Minimum Curvature algorithm was used to interpolate values onto a rectangular regular spaced grid.

The magnetic derivative analyses were obtained using algorithms developed inside the Geosoft Mapmap ™ platform. The FFT based analyses were performed directly on the Geosoft grids of the final corrected total magnetic intensity data.

5. DELIVERABLES

5.1 Survey Report

The survey report describes the data acquisition, processing, and final presentation of the survey results. The survey report is provided in two paper copies and digitally in PDF format.

5.2 Maps

Final maps were produced at a scale of 1:20,000 and 1:10,000. The coordinate/projection system used was NAD83, UTM zone 16 north. All maps show the flight path trace and topographic data; latitude and longitude are also noted on maps.

The preliminary and final results of the survey are presented as EM profiles, a late-time gate gridded EM channel, and color magnetic TMI contour maps.

The following maps are presented on paper:

- VTEM B-field profiles, Time Gates 0.234 – 6.578 ms in linear - logarithmic scale with TMI colour image.
- VTEM dB/dt profiles, Time Gates 0.234 – 6.578 ms in linear – logarithmic scale.
- VTEM B-field late time, Time Gate 1.953 ms colour image.
- Total magnetic intensity (TMI) colour image and contours.
- VTEM B-Field & dB/dt Calculated Time Constant (TAU) colour image.
- Calculated Magnetic Vertical Derivative colour image.

5.3 Digital Data

- Two copies of the data and maps on DVD-ROM were prepared to accompany the report. Each DVD -ROM contains a digital file of the line data in GDB Geosoft Montaj format as well as the maps in Geosoft Montaj Map format.

- Two copies of DVD-ROMs were prepared.

There are two (2) main directories:
Data contains databases, grids and maps, as described below.
Report contains a copy of the report and appendices in PDF format.

Databases in Geosoft GDB format containing the channels listed, are presented in Table 5.

Table 5 - Geosoft GDB Data Format

Channel Name	**Description**
X:	X positional data (meters – NAD83, UTM zone16 north)
Y:	Y positional data (meters – NAD83, UTM zone 16 north)
Z:	GPS antenna elevation (meters - ASL)
Radar:	Helicopter terrain clearance from radar altimeter (meters - AGL)
RadarB:	EM Bird terrain clearance from radar altimeter (meters - AGL)
DEM:	Digital elevation model (meters)
Gtime:	GPS time (seconds of the day)
Mag1:	Raw Total Magnetic field data (nT)
Mag2:	Diurnal corrected Total Magnetic field data (nT)
Mag3:	Leveled Total Magnetic field data (nT)
Basemag:	Magnetic diurnal variation data (nT)
SF[10]:	dB/dt 120 microsecond time channel (pV/Am^4)
SF[11]:	dB/dt 141 microsecond time channel (pV/Am^4)
SF[12]:	dB/dt 167 microsecond time channel (pV/Am^4)
SF[13]:	dB/dt 198 microsecond time channel (pV/Am^4)
SF[14]:	dB/dt 234 microsecond time channel ($pV/A/m^4$)
SF[15]:	dB/dt 281 microsecond time channel (pV/Am^4)
SF[16]:	dB/dt 339 microsecond time channel (pV/Am^4)
SF[17]:	dB/dt 406 microsecond time channel (pV/Am^4)
SF[18]:	dB/dt 484 microsecond time channel (pV/Am^4)
SF[19]:	dB/dt 573 microsecond time channel (pV/Am^4)
SF[20]:	dB/dt 682 microsecond time channel (pV/Am^4)
SF[21]:	dB/dt 818 microsecond time channel (pV/Am^4)
SF[22]:	dB/dt 974 microsecond time channel (pV/Am^4)
SF[23]:	dB/dt 1151 microsecond time channel (pV/Am^4)
SF[24]:	dB/dt 1370 microsecond time channel (pV/Am^4)
SF[25]:	dB/dt 1641 microsecond time channel (pV/Am^4)
SF[26]:	dB/dt 1953 microsecond time channel (pV/Am^4)
SF[27]:	dB/dt 2307 microsecond time channel (pV/Am^4)
SF[28]:	dB/dt 2745 microsecond time channel (pV/Am^4)
SF[29]:	dB/dt 3286 microsecond time channel (pV/Am^4)
SF[30]:	dB/dt 3911 microsecond time channel (pV/Am^4)
SF[31]:	dB/dt 4620 microsecond time channel (pV/Am^4)
SF[32]:	dB/dt 5495 microsecond time channel (pV/Am^4)
SF[33]:	dB/dt 6578 microsecond time channel (pV/Am^4)
BF[10]:	B-field 120 microsecond time channel $(pVms)/(Am^4)$
BF[11]:	B-field 141 microsecond time channel $(pVms)/(Am^4)$

Channel Name	Description
BF[12]:	B-field 167 microsecond time channel (pVms)/(Am^4)
BF[13]:	B-field 198 microsecond time channel (pVms)/(Am^4)
BF[14]:	B-field 234 microsecond time channel (pVms)/(Am^4)
BF[15]:	B-field 281 microsecond time channel (pVms)/(Am^4)
BF[16]:	B-field 339 microsecond time channel (pVms)/(Am^4)
BF[17]:	B-field 406 microsecond time channel (pVms)/(Am^4)
BF[18]:	B-field 484 microsecond time channel (pVms)/(Am^4)
BF[19]:	B-field 573 microsecond time channel (pVms)/(Am^4)
BF[20]:	B-field 682 microsecond time channel (pVms)/(Am^4)
BF[21]:	B-field 818 microsecond time channel (pVms)/(Am^4)
BF[22]:	B-field 974 microsecond time channel (pVms)/(Am^4)
BF[23]:	B-field 1151 microsecond time channel (pVms)/(Am^4)
BF[24]:	B-field 1370 microsecond time channel (pVms)/(Am^4)
BF[25]:	B-field 1641 microsecond time channel (pVms)/(Am^4)
BF[26]:	B-field 1953 microsecond time channel (pVms)/(Am^4)
BF[27]:	B-field 2307 microsecond time channel (pVms)/(Am^4)
BF[28]:	B-field 2745 microsecond time channel (pVms)/(Am^4)
BF[29]:	B-field 3286 microsecond time channel (pVms)/(Am^4)
BF[30]:	B-field 3911 microsecond time channel (pVms)/(Am^4)
BF[31]:	B-field 4620 microsecond time channel (pVms)/(Am^4)
BF[32]:	B-field 5495 microsecond time channel (pVms)/(Am^4)
BF[33]:	B-field 6578 microsecond time channel (pVms)/(Am^4)
Lon:	Longitude data (degree – NDA83)
Lat:	Latitude data (degree – NAD83)
PLM:	60 Hz power line monitor
TauSF:[8]	Time Constant (Tau) calculated from dB/dt data (mSec)
TauBF:	Time Constant (Tau) calculated from B-field data (mSec)

Electromagnetic B-field and dB/dt data are found in array channel format between indexes 10 – 33, as described above.

[8] An explanation of the VTEM time constant is given in Appendix F.

- Database of the VTEM Waveform "8218_waveform.gdb" in Geosoft GDB format, containing the following channels:

Time:	Sampling rate interval, 10.416 microseconds
RX_Volt:	Output voltage of the receiver coil (volt)
TX_Curr:	Output current of the transmitter (amps)

- Grids in Geosoft GRD format, as follow,

Mag3_bb.grd:	Total magnetic intensity (nT)
BF26_bb:	B-Field Time Gate 1.953 ms
CVG_bb:	Calculated Magnetic Vertical Derviative
TAUbf_bb:	Calculated Time Constant (TAU)
TAUsf_bb:	Calculated Time Constant (TAU)

Where bb represents the block name (ie: 8218_mag_TwinFalls).

A Geosoft .GRD file has a .GI metadata file associated with it, containing grid projection information. A grid cell size of 25 metres was used.

- Maps at 1:20,000 and 1:10,000 scale in Geosoft MAP format, as follows:

8218_TMI_bb:	B-field profiles, Time Gates 0.234 – 6.578 ms in linear logarithmic scale, with TMI colour image.
8218_dBdt_bb:	dB/dt profiles, Time Gates 0.234 – 6.578 ms in linear logarithmic scale.
8218_BF26_bb:	B-field late time, Time Gate 1.953 ms colour image.
8218_TMI_bb:	Total magnetic intensity colour image and contours.
8218_CVD_bb:	Calculated Magnetic Vertical Derivative
8218_TAUBF_bb:	B-Field Calculated Time Constant (TAU)
8218_TAUSF_bb:	dB/dt Calculated Time Constant (TAU)

Where bb represents the block name (ie: 8218_BF26_TwinFalls).

1:50,000 topographic vectors were taken from the NRCAN Geogratis database at; http://geogratis.gc.ca/geogratis/en/index.html.

- Google Earth files *8218_Kodiak.kml* showing the flight path of the block.

Free version of Google Earth software can be downloaded from, http://earth.google.com/download-earth.html

6. PRELIMINARY INTERPRETATION

6.1 Geological Context and Mineralization

The surveyed blocks geologically belong to Beardmore-Geraldon deformed greenstone belt located between the multi-million ounce Red Lake and Timmins gold camps.

Greenstone-hosted quartz–carbonate vein gold mineralization is structurally controlled along faults, shear zones and associated with large scale iron-carbonate alteration trends commonly distributed along major fault zones and subsidiary structures[9]. This type of gold deposit is characterized by moderately to steeply dipping, laminated fault-fill quartz-carbonate veins which typically infill the central part of, and are subparallel to slightly oblique to, the host structures (see Figure from Dubé, and Gosselin, 2007, below).

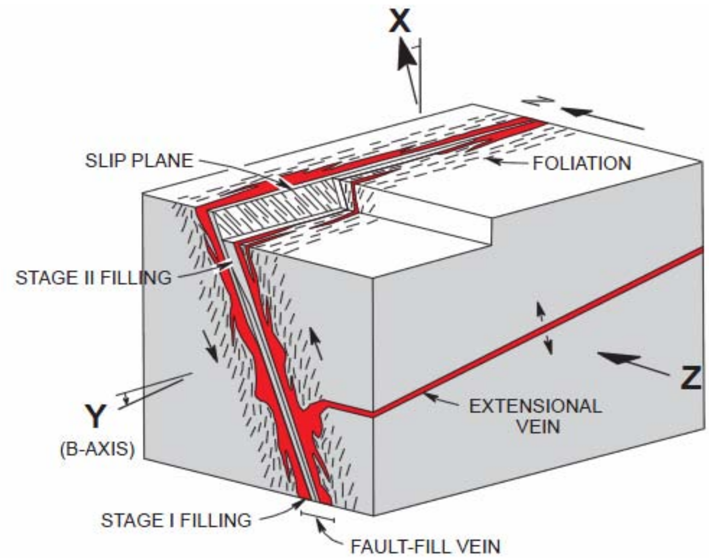

FIGURE 1. Schematic diagram illustrating the geometric relationships between the structural element of veins and shear zones and the depositscale strain axes (from Robert, 1990).

Individual vein thickness varies from a few centimeters up to 5 meters. Gold mineralized systems in the district have been exposed over a strike length of more than 1.2 kilometers.

Typically, the alteration haloes are zoned and characterized – in rocks at green schist facies – by iron-carbonatization and sericitization, with sulphidation of the immediate vein selvages (mainly pyrite, arsenopyrite). Gold is mainly confined to the quartz-carbonate vein networks but may also be present in significant amounts within iron-rich sulphidized wall-rock selvages or within silicified and arsenopyrite-rich replacement zones.

As a rule greenstone-hosted quartz-carbonate vein deposits are associated with mafic and ultramafic rocks including sills and dykes of the rocks.

On a deposit scale, exploration models of the kind of gold deposits include key elements in locating the richest parts such as structural traps – fold hinges or dilational jogs along faults or shear zones, or veins. Geometric ore shoots are controlled by the intersection of the given structures with favorable lithological units such as a competent gabbroic sill, a dyke, an iron formation, or a particularly reactive rock.

---

9 Dubé, B., and Gosselin, P., 2007, Greenstone-hosted quartz-carbonate vein deposits, in Goodfellow, W.D., ed., Mineral Deposits of Canada: A Synthesis of Major Deposit-Types, District Metallogeny, the Evolution of Geological Provinces, and Exploration Methods: Geological Association of Canada, Mineral Deposits Division, Special Publication No.5, p49-73.

6.2 Possible Principles of Interpretation and Analysis of the Geophysical Data

According to the geological model of gold producing zones it is very important for the region and the type of gold mineralization to find out where are the potential gold producing structures. Because the structures are often accompanied by alteration zones with conductive minerals, EM methods can be used as targeting tools.

Then EM response due to subvertical thin targets typically produce double peak anomalies (Figure 7).

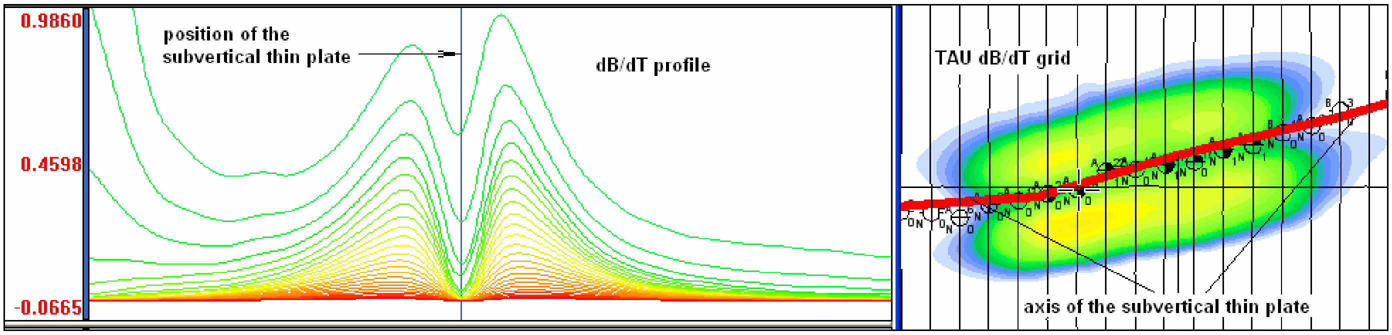

Figure 7 - EM response from subvertical thin plate target (Lattimer block)

The posted EM anomaly centers on all maps are related to projection of the top of the sources on surface and indicate the conductor axes.

A schematic map of the potential productive structures on basis of VTEM results for Lattimer-Solo-Maki block is shown in Figure 8 together with Calculated Vertical Magnetic Derivative (CVG) grid which highlights very well shallow magnetic source features. These are probably related to a mafic or ultramafic formations.

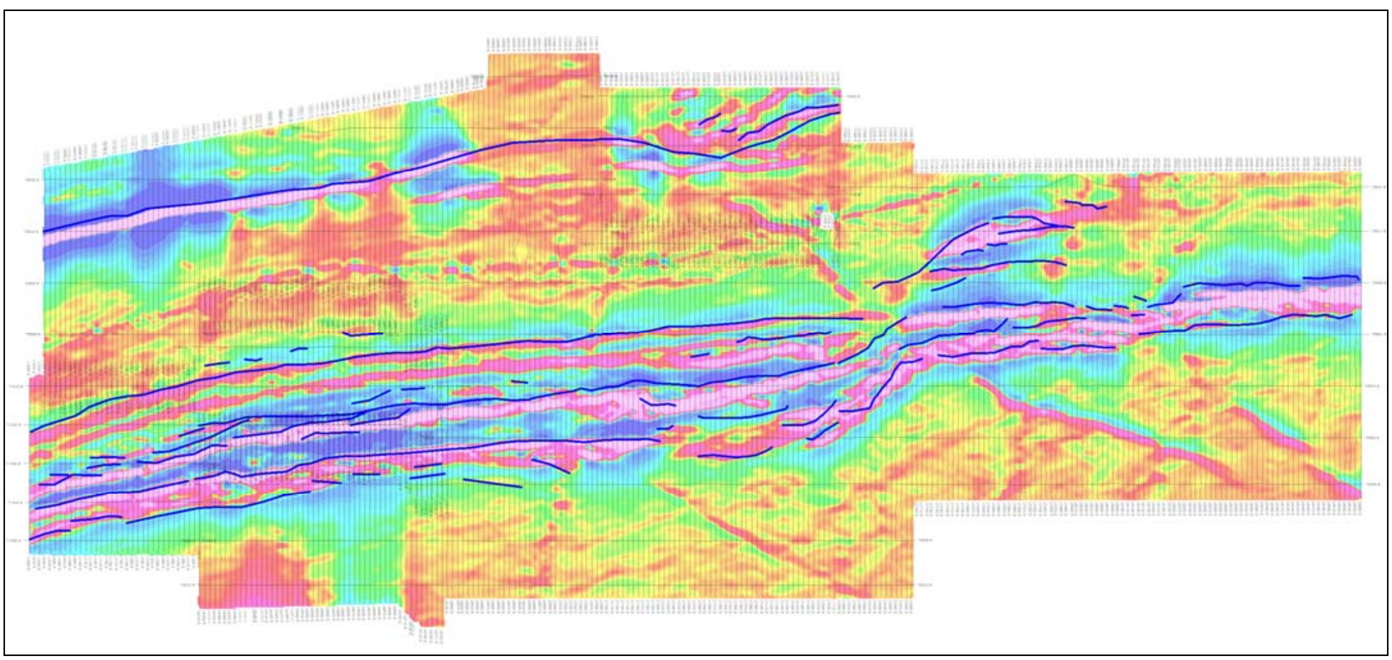

Figure 8 - Axes of conductive subvertical zones with CVG grid. Lattimer-Solo-Maki block.

Combined analysis of magnetic and EM fields and their derivatives can provide the finding of perspective structural traps:

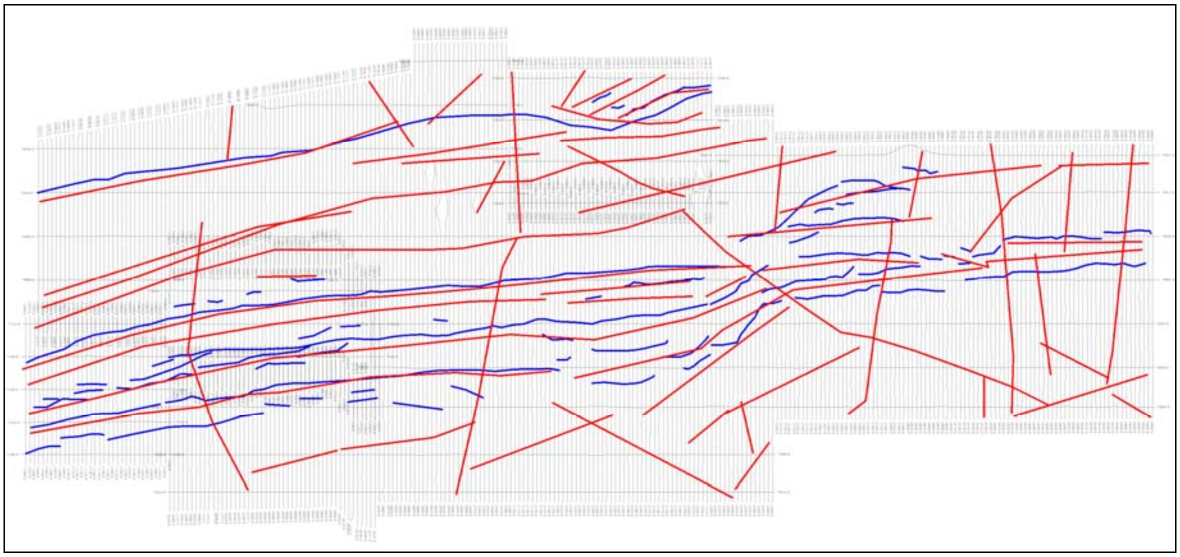

Figure 9 - Axes of conductive zones (blue lines) and linear features of magnetic field (red lines). Lattimer-Solo-Maki block.

Finally for more detailed analyses and drill-planning, 2.5D modeling should be used. The conductive faults and shear zones have different directions and dips in different parts of the area. First of all it is important to determine depth and direction for planning drillholes and secondly this feature could be important for location of possible productive mineralization (foot wall or hanging wall).

For example a 2.5D model of one of conductive zones is presented in Figure 10:

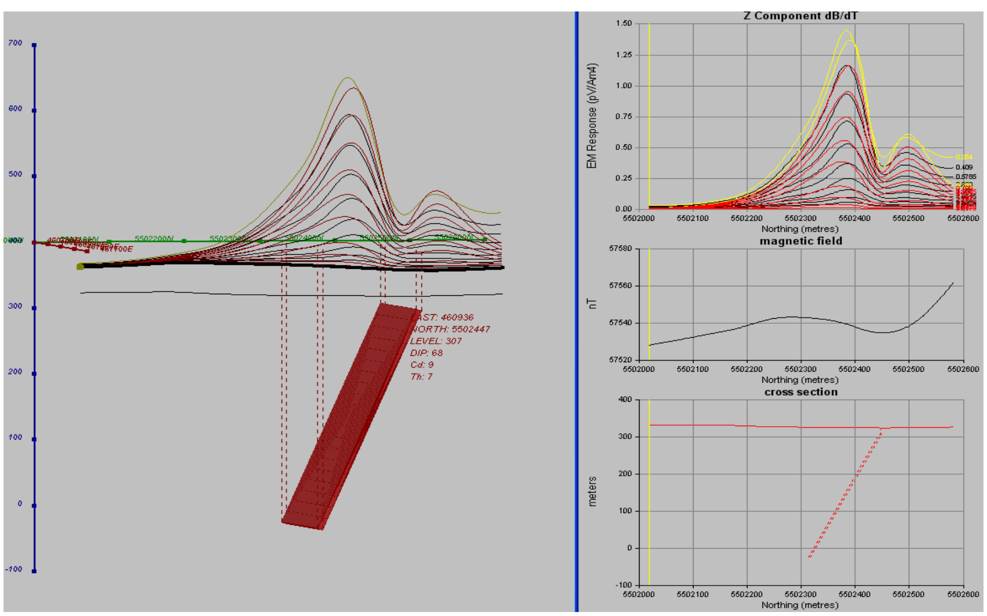

Figure 10 - Results of the modeling of EM anomaly on 7910 line of east part of Lattimer block.

7. CONCLUSIONS AND RECOMMENDATIONS

7.1 Conclusions

A helicopter-borne versatile time domain electromagnetic (VTEM) geophysical survey has been completed over 7 blocks near the town of Beardmore, Ontario, Canada.

The total area coverage is 485.9km^2. Total survey line coverage is 4964 line kilometres. The principal sensors included a Versatile Time Domain EM system and caesium magnetometer. Results have been presented as stacked profiles and colour contour images at a scale of 1:20,000 and 1:10,000.

The geophysical results are briefly discussed and interpreted using EM anomaly picking and time constant (Tau) analysis,as well as magnetic derivative analysis.

7.2 Recommendations

Based on the geophysical results obtained, a number of potentially interesting EM and magnetic anomalies were identified on the property. We therefore recommend that these results be combined and compared with the existing geoscientific database. We further recommend a more detailed interpretation of the EM and magnetic data including 2.5D inversion and modelling techniques to better characterize them and to more accurately determine the anomaly parameters (depth, conductance, dip, etc.) prior to ground follow-up and drill testing.

Respectfully submitted[1],

Wendy Acorn
Geotech Ltd.

Jean Legault, P. Geo, P. Eng
Geotech Ltd.

Alex Prikhodko
Geotech Ltd.

December 2008

[1]Final data processing of the EM and magnetic geophysical data were carried out by Alex Prikhodko from the office of Geotech Ltd., in Aurora, Ontario, under the supervision of Jean Legault, P. Geo, Manager of Data Processing and Interpretation.

APPENDIX A

SURVEY BLOCK LOCATION MAP

Google Earth Location map of Blocks

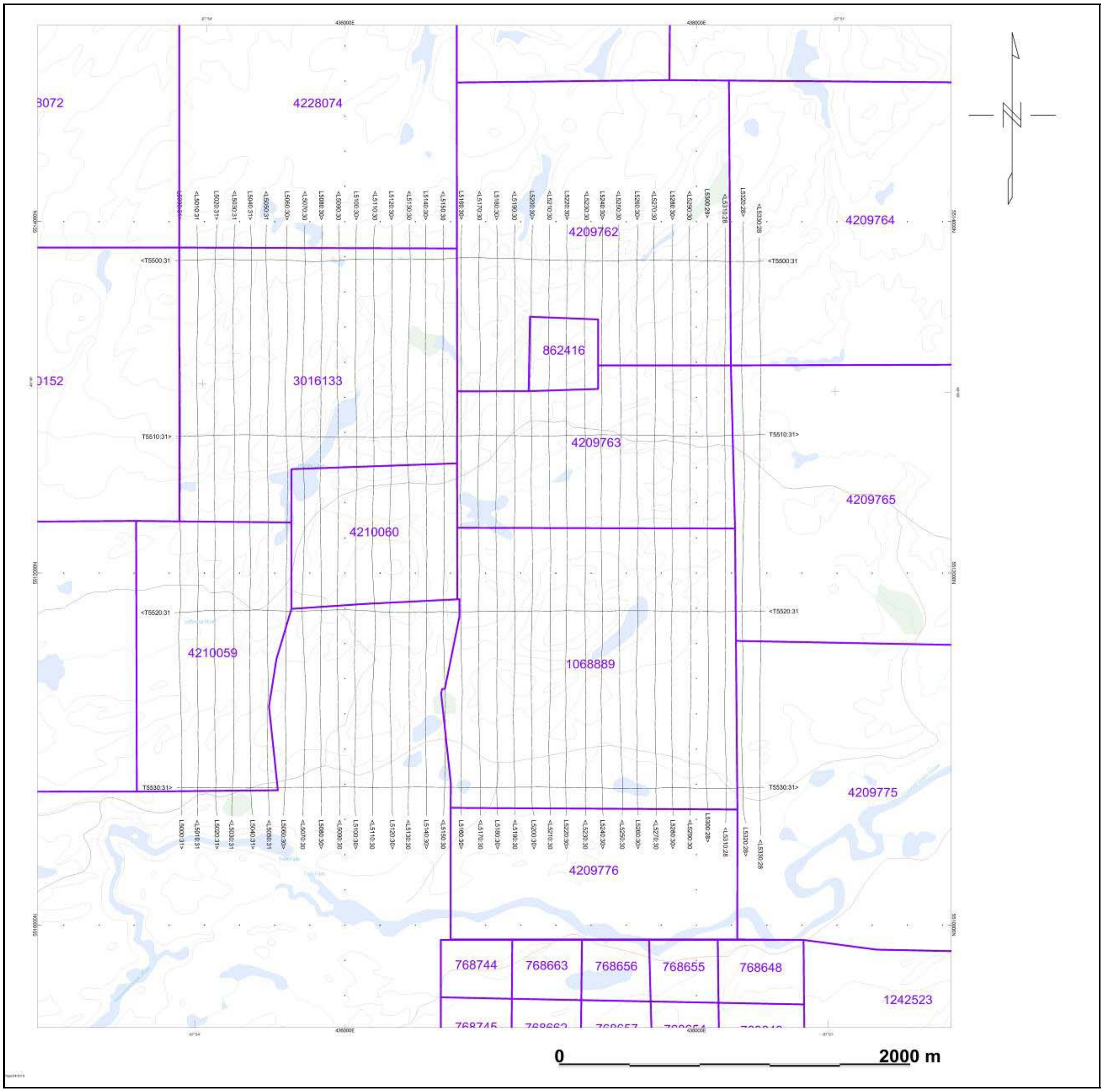

Mining Claims map for the Twin Falls Block

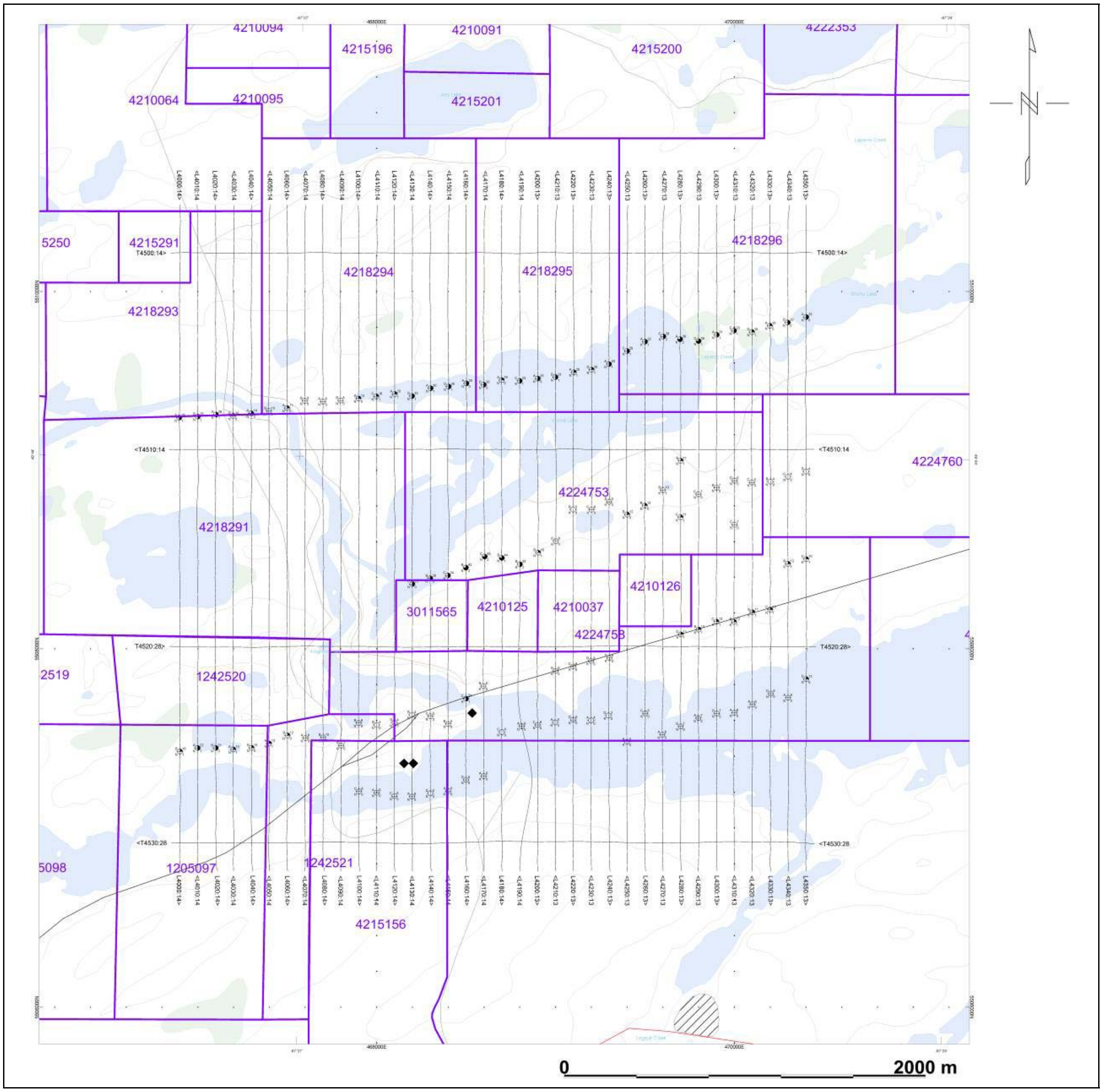

Mining Claims map for the St Bridge Block

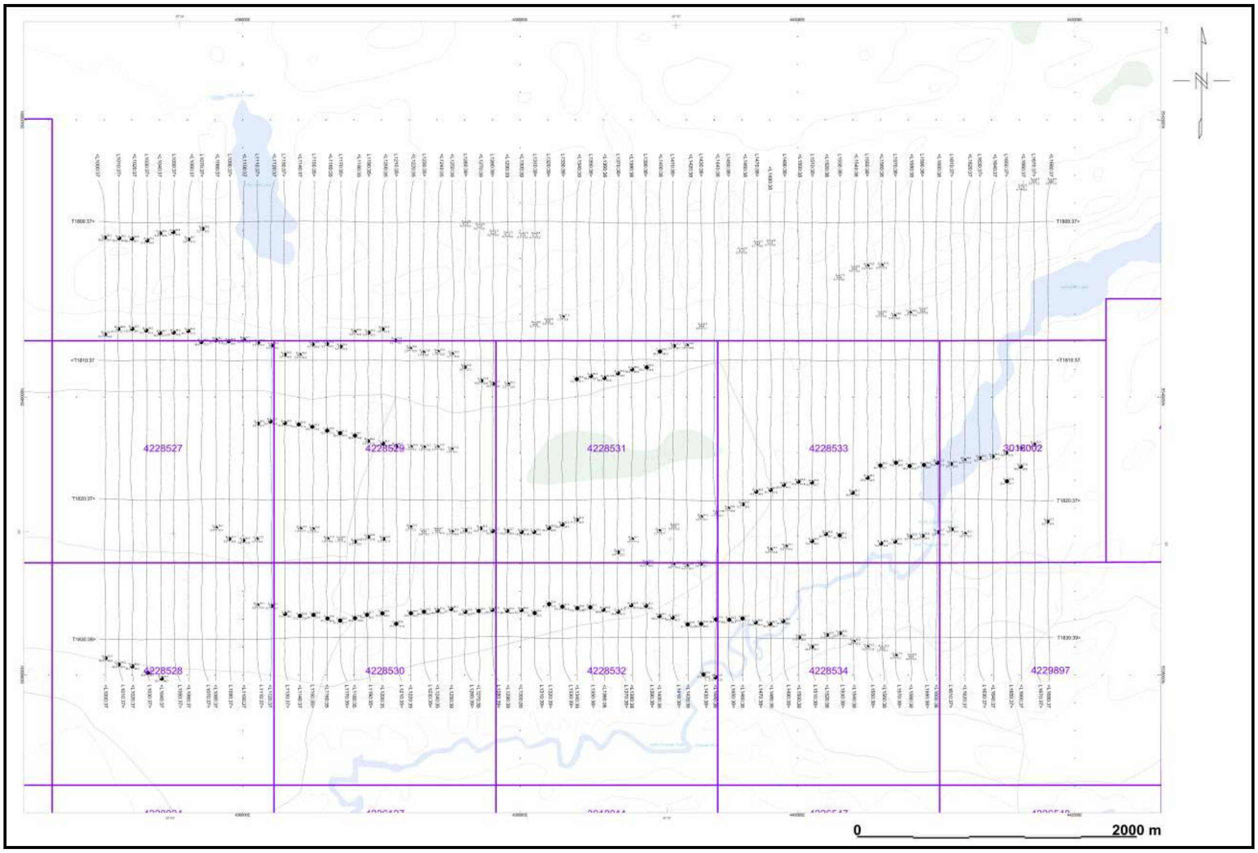

Mining Claims map for the Little John Block

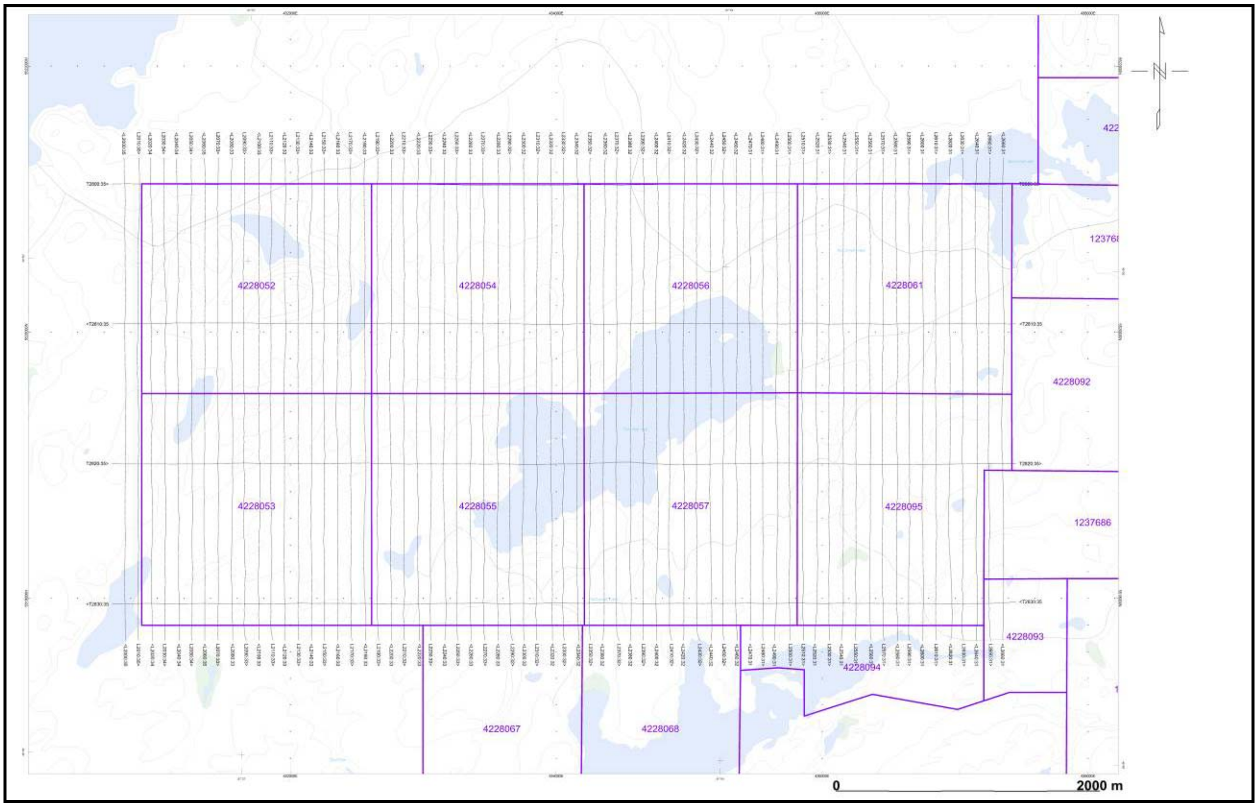

Mining Claims map for the Forge Creek Block

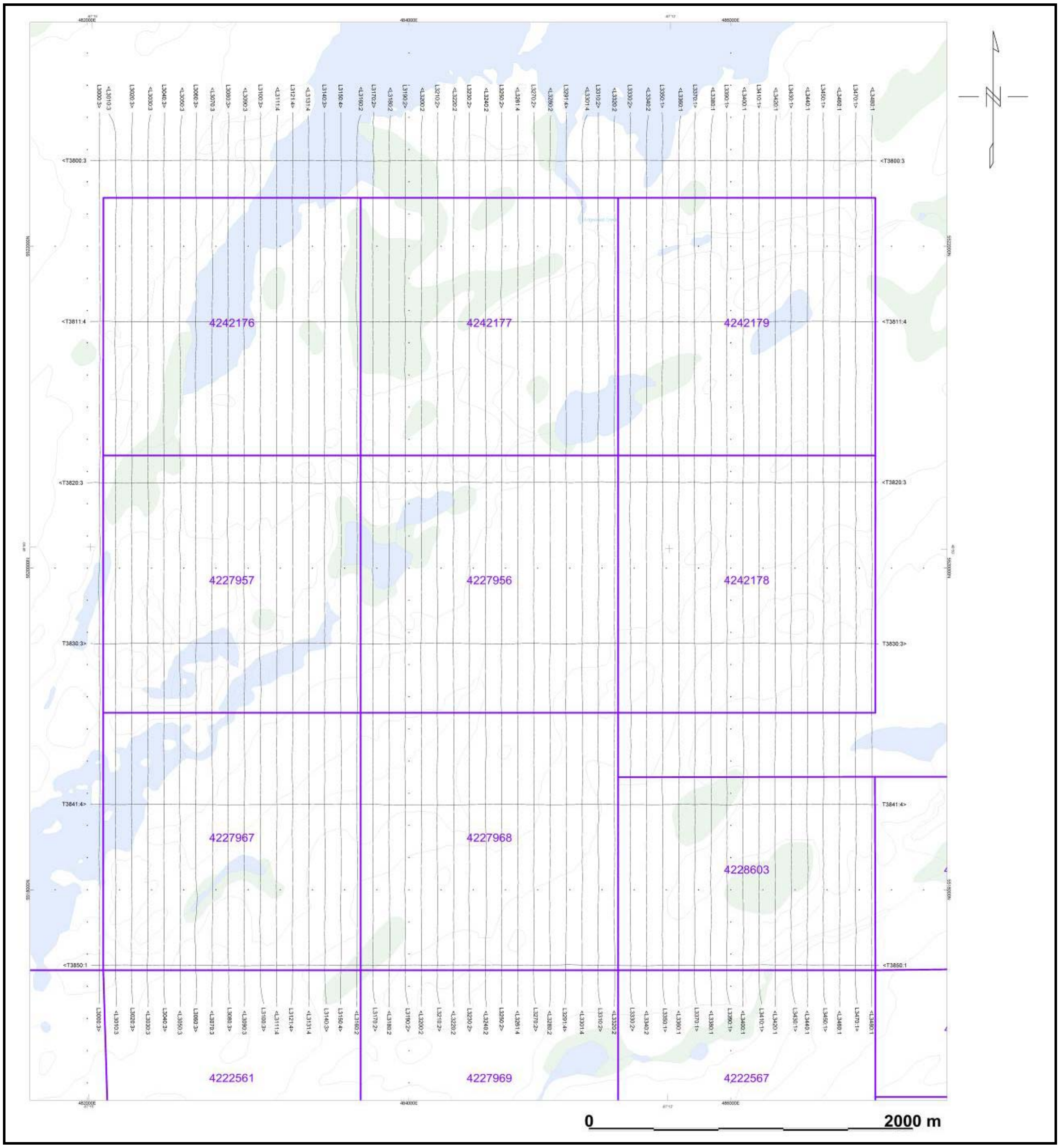

Mining Claims map for the NIK Block

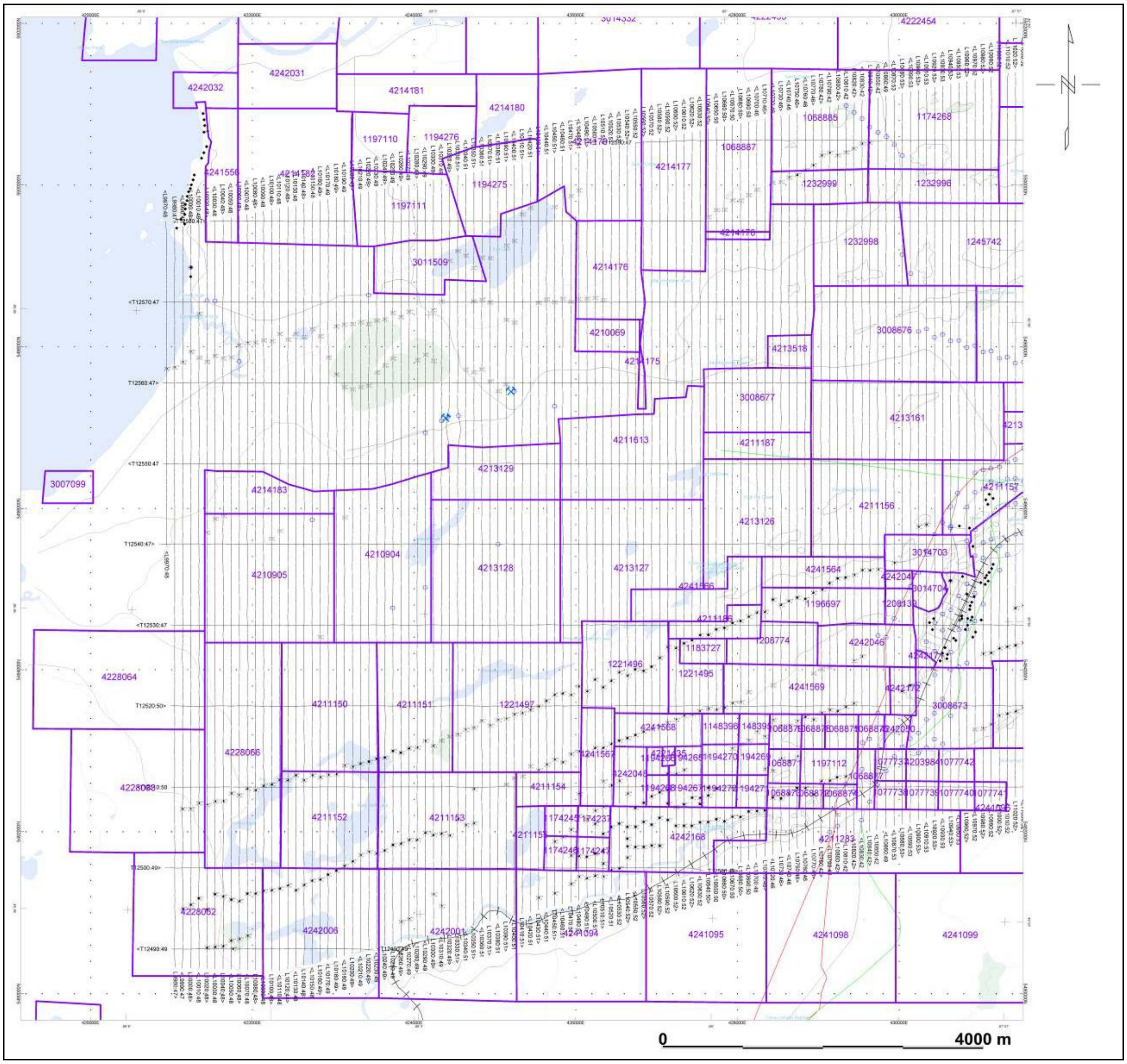

Mining Claims map for the Empire (east end) Block

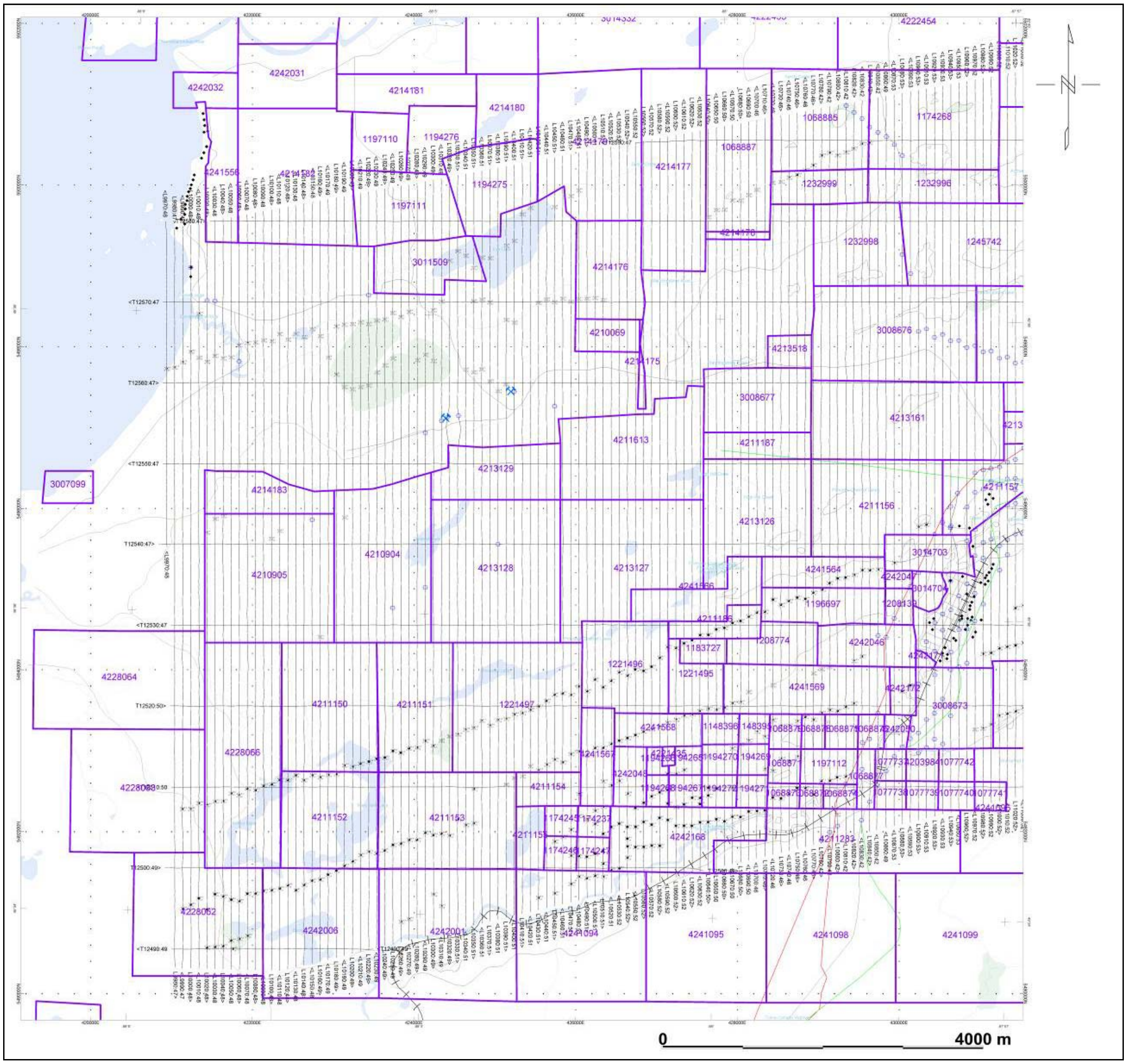

Mining Claims map for the Empire (west end) Block

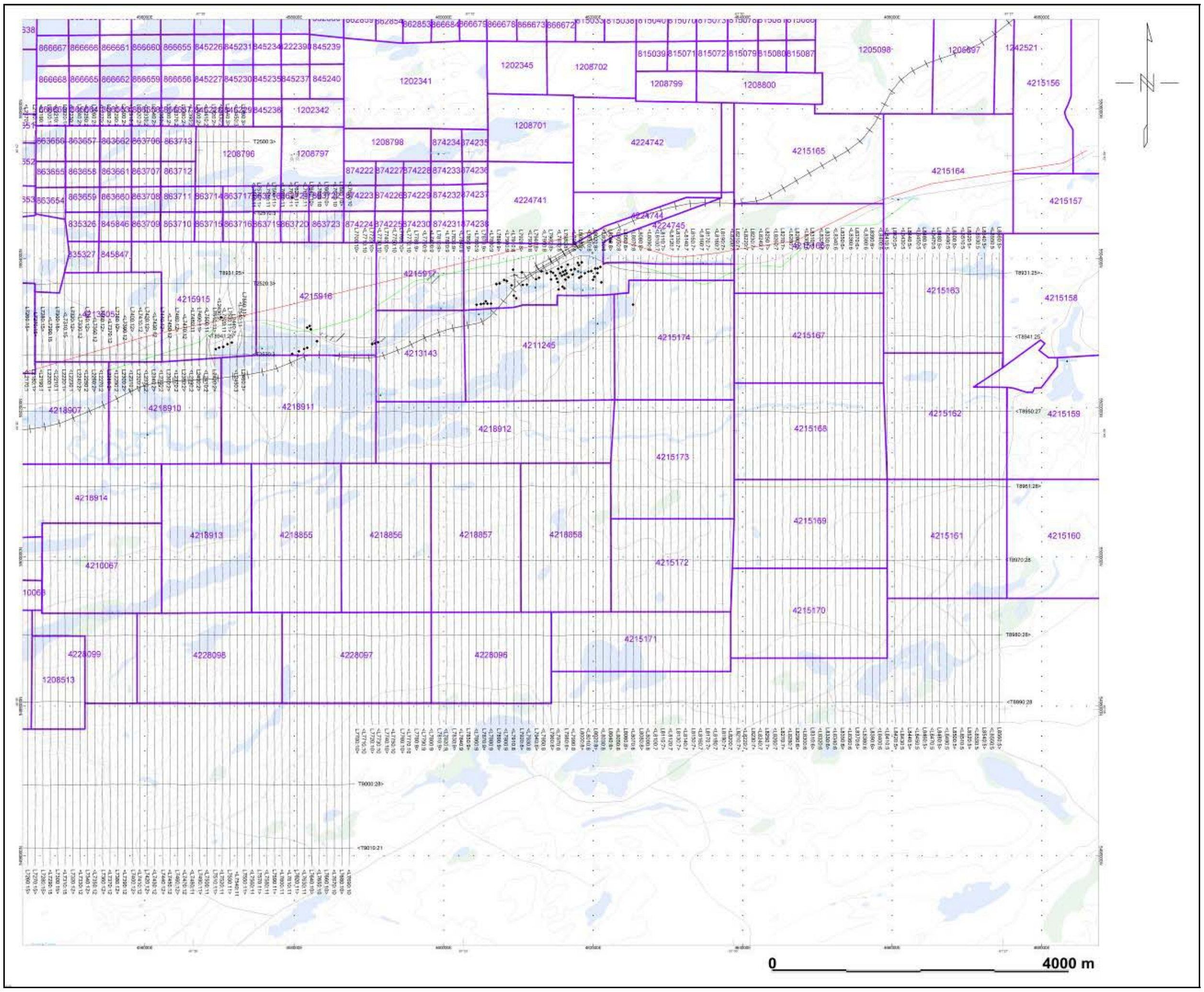

Mining Claims map for the Lattimer (east end) Block

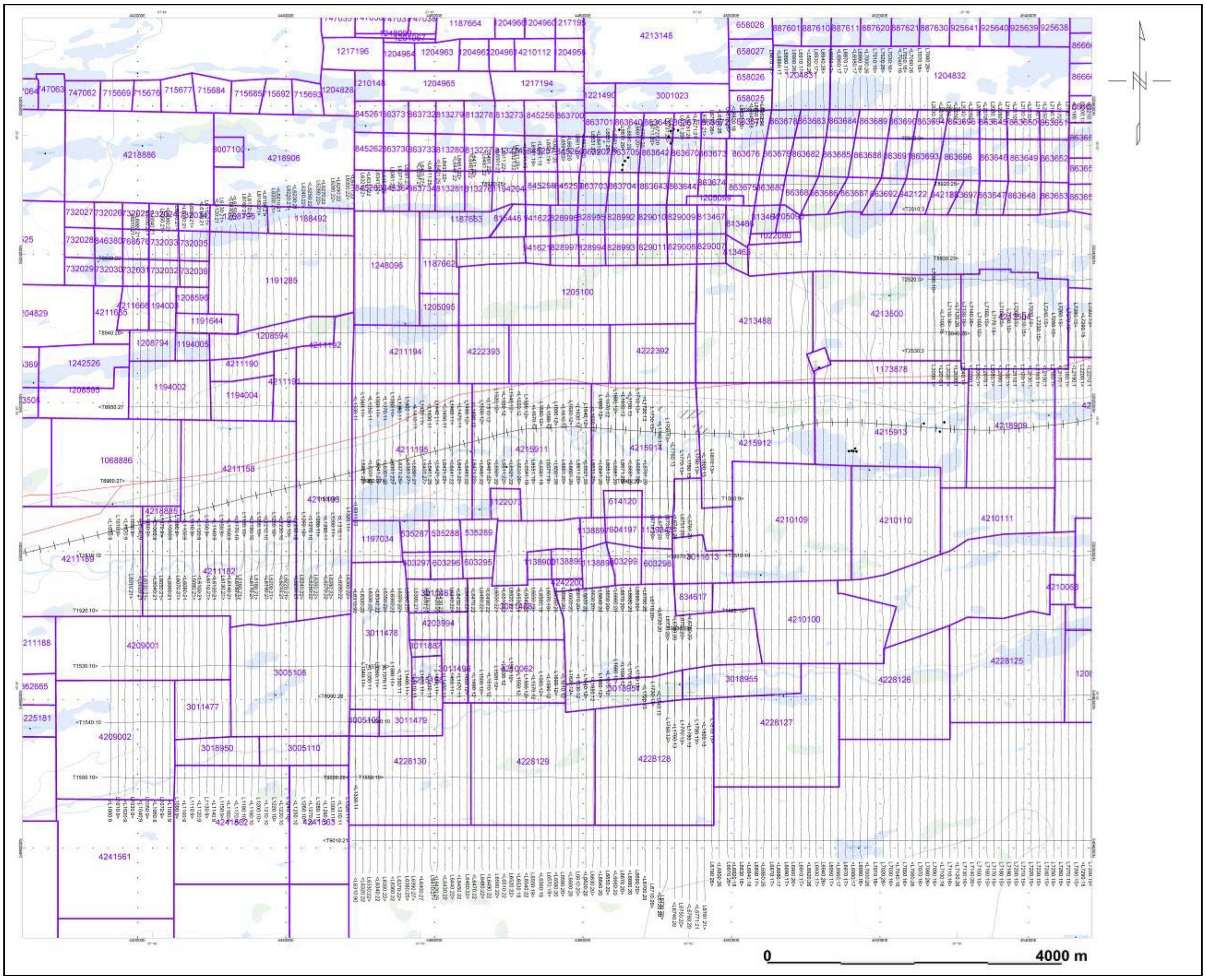

Mining Claims map for the Lattimer (west end) Block

APPENDIX B

SURVEY BLOCK COORDINATES

(NAD83 zone 16north)

Empire

X	Y
441834.5	5503214
441576.6	5494699
436197.8	5492840
432439.9	5492765
422345.4	5490386
420982.2	5490423
420908.6	5499347

St Bridge

X	Y
466900.1	5510315
470419.2	5510315
470419.2	5506854
466900.1	5506854

Forge Creek

X	Y
430756.8	5521210
437371.5	5521210
437371.5	5517783
430756.8	5517783

Little John

X	Y
435005.4	5541363
441815.4	5541363
441815.4	5538153
435005.4	5538153

Lattimer

X	Y
441905.7	5499987
441905.7	5503813
441832.3	5503898
450618	5505457
450618	5506137
452695.6	5506145
452665.4	5502749
457401	5502712
457401	5504411
458808.5	5504437
458723.5	5503870
467452.4	5503870
467452.4	5497918
458780.2	5497918
458780.2	5495991
444864.8	5495991
444866.1	5498746
448876.2	5498737
448876.2	5498410
449212.6	5498401
449186	5497931
449743.7	5497931
449726	5500773
449177.2	5500764
449194.9	5501145
448867.3	5501154
448876.2	5501455
444857.2	5501446
444864.8	5499987

NIK

X	Y
482076.2	5522632
486929.7	5522632
486929.7	5517472
482076.2	5517472

Twin Falls

X	Y
435064	5513882
438398.4	5513882
438398.4	5510722
435064	5510722

APPENDIX C

VTEM WAVEFORM

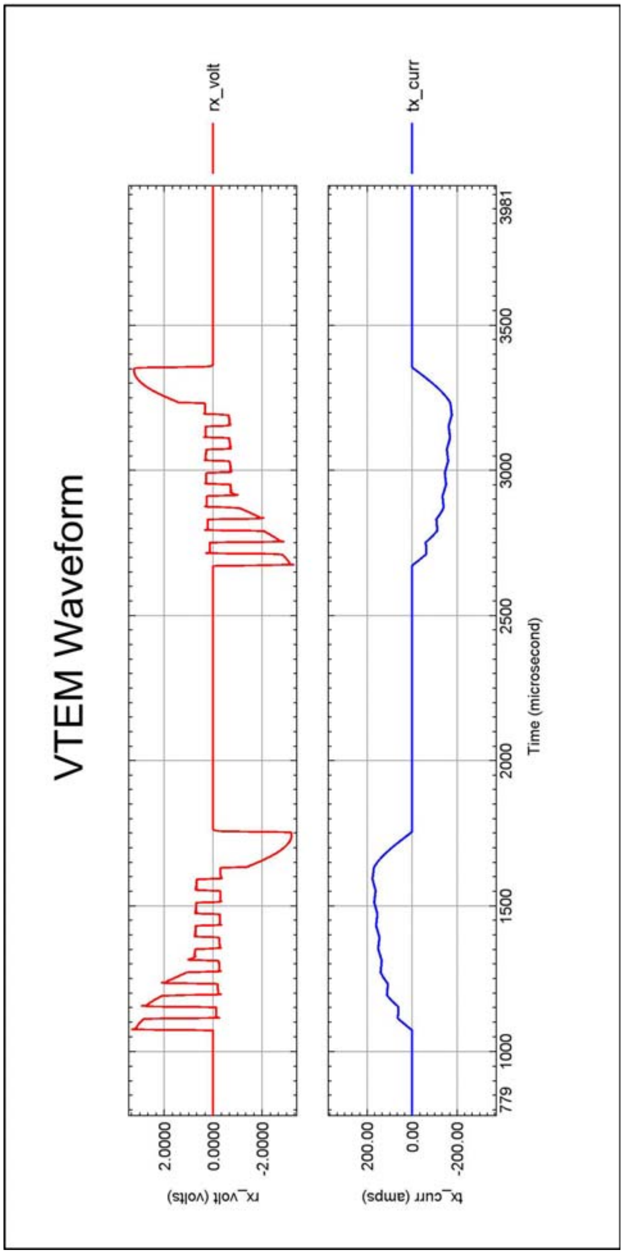

APPENDIX D

GEOPHYSICAL MAPS[10]

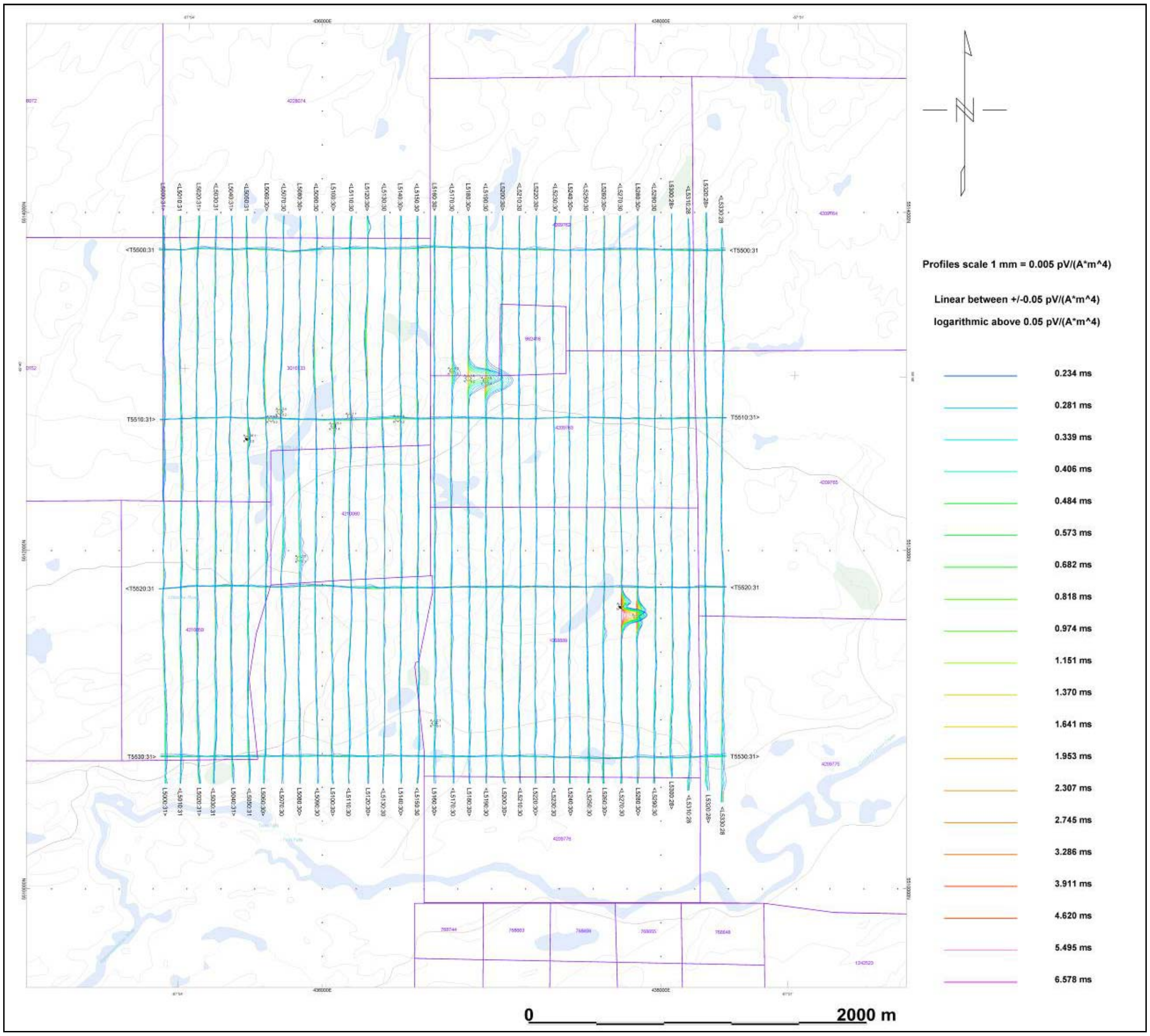

VTEM dB/dt Profiles for the Twin Falls Block with EM anomalies

[10] Present maps are a selection of the final geophysical maps. Full size geophysical maps are also available in PDF format on the final DVD.

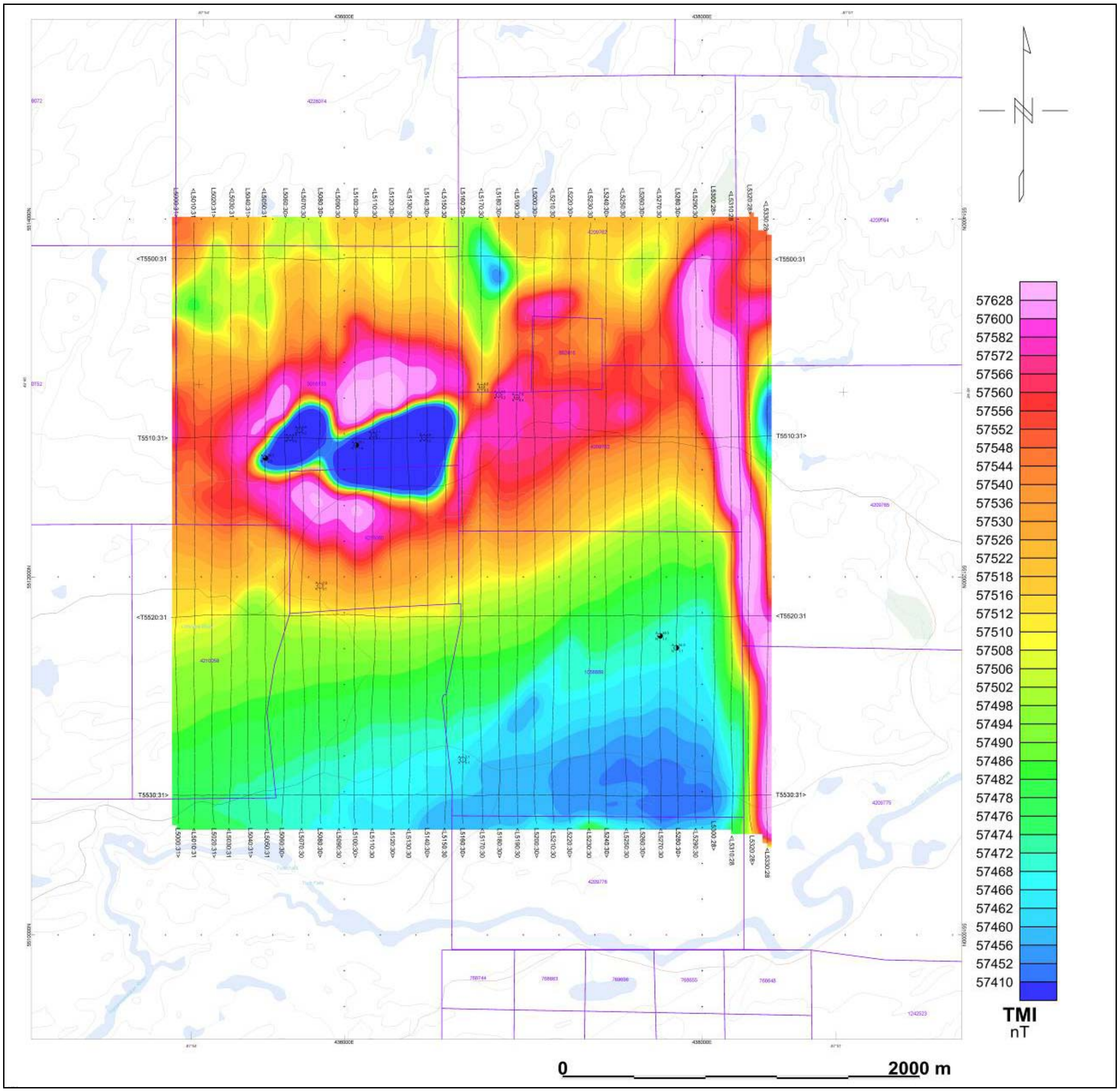

Total Magnetic Intensity (TMI) Grid for the Twin Falls Block with EM anomalies

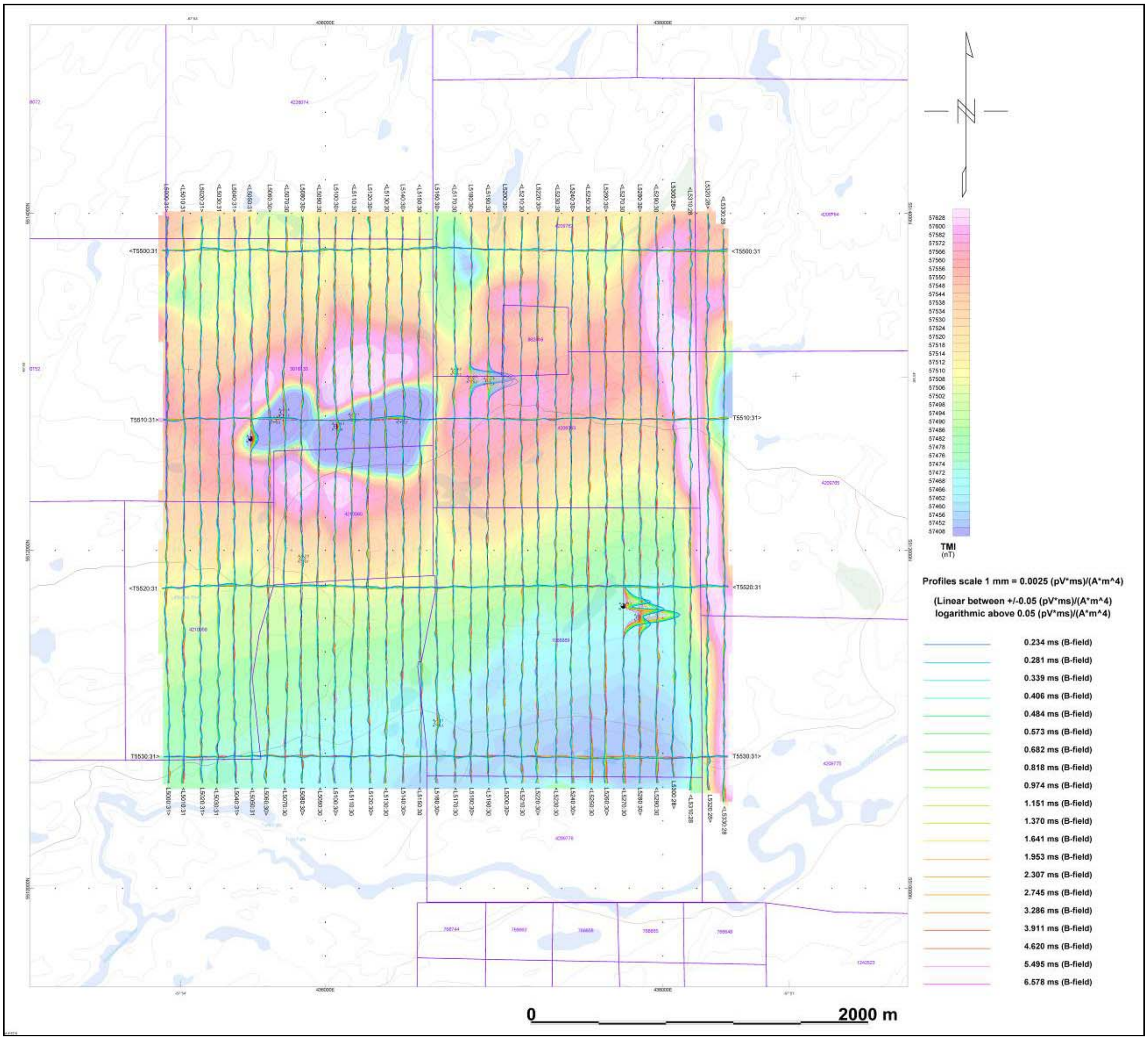

VTEM B-Field Profiles with TMI Color Image for the Twin Falls Block with EM anomalies

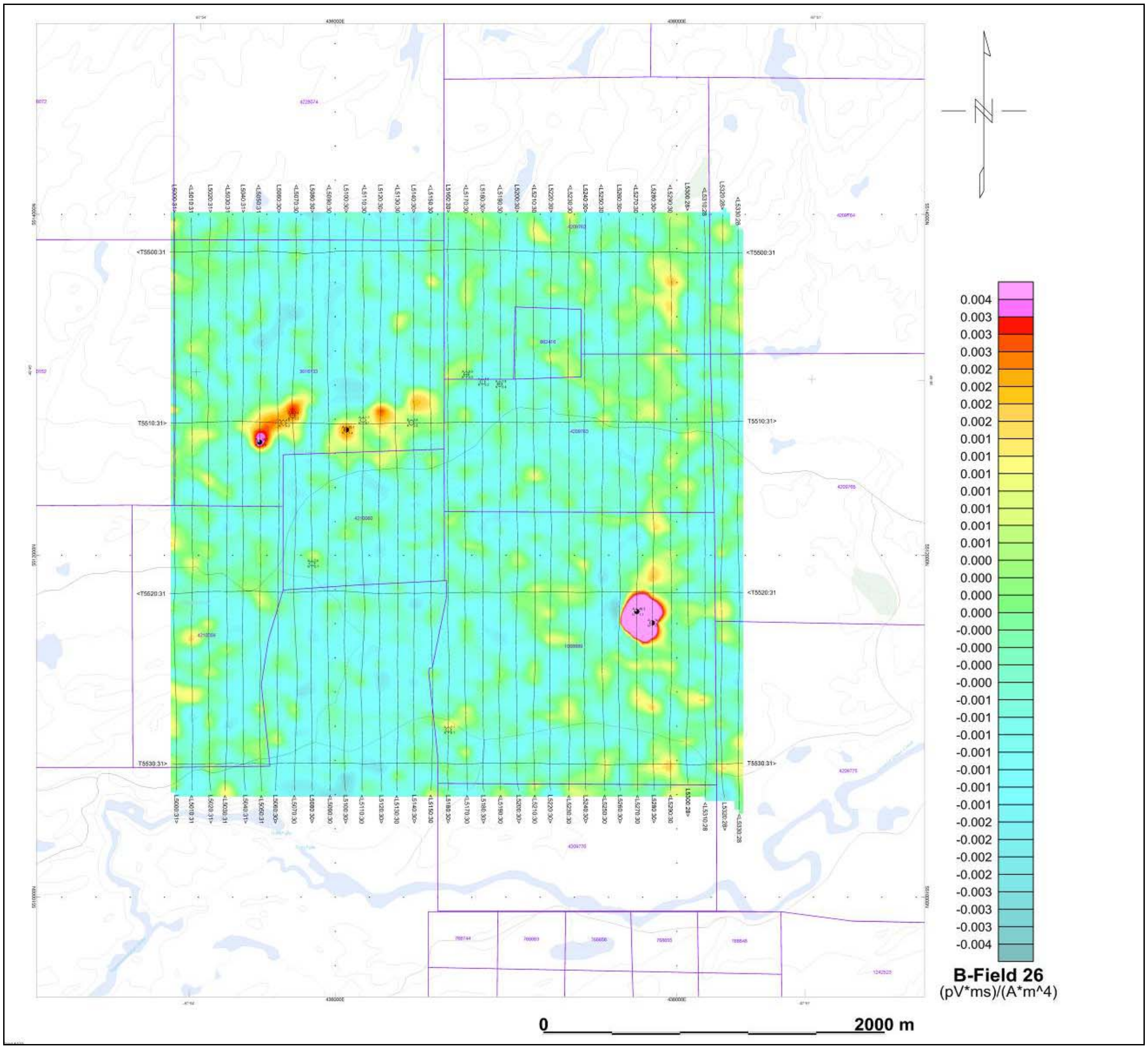

VTEM B-Field Grid - Time Gate 1.151 ms for the Twin Falls Block with EM anomalies

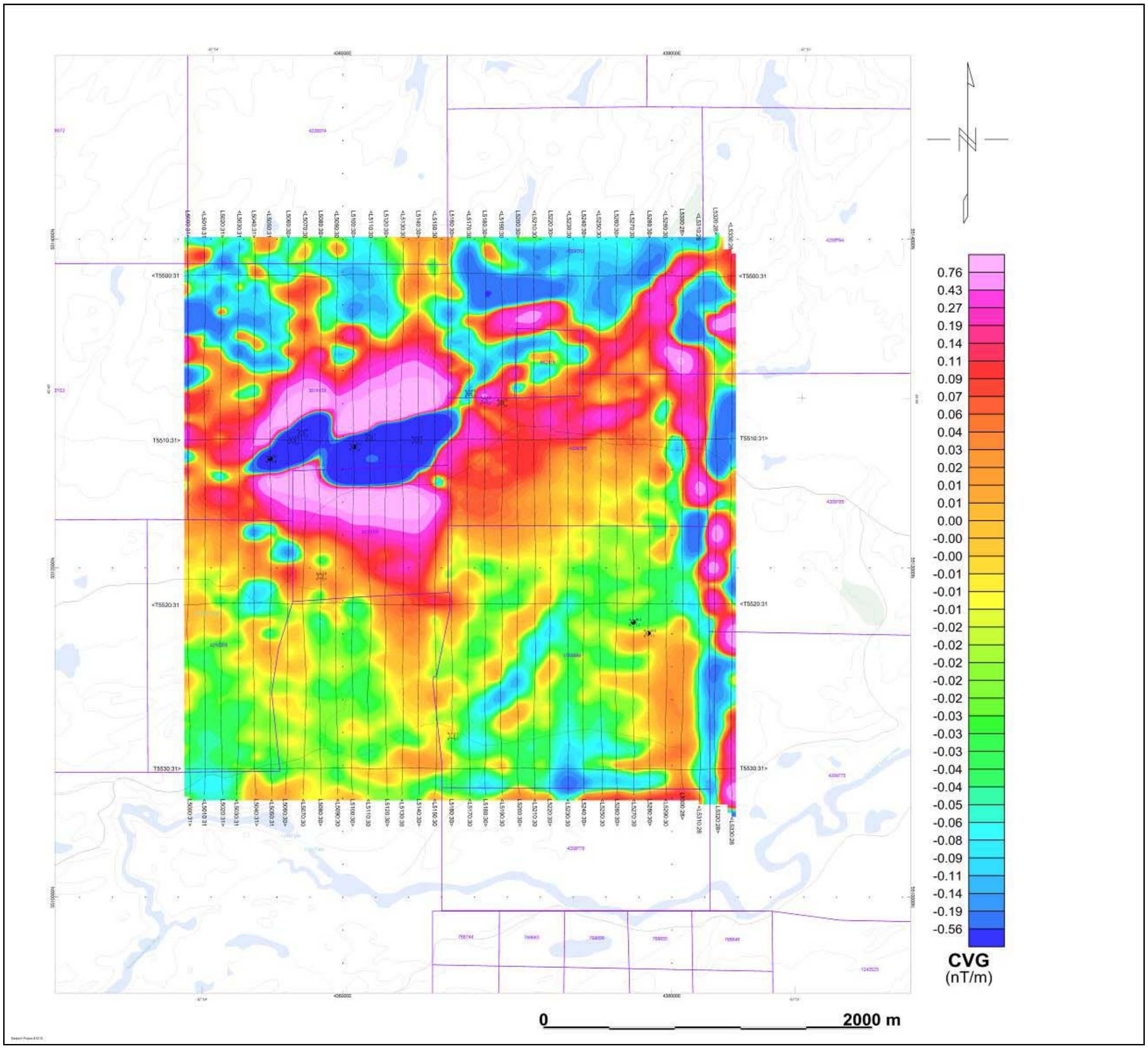

Calculated Magnetic Vertical Derivative for the Twin Falls Block with EM anomalies

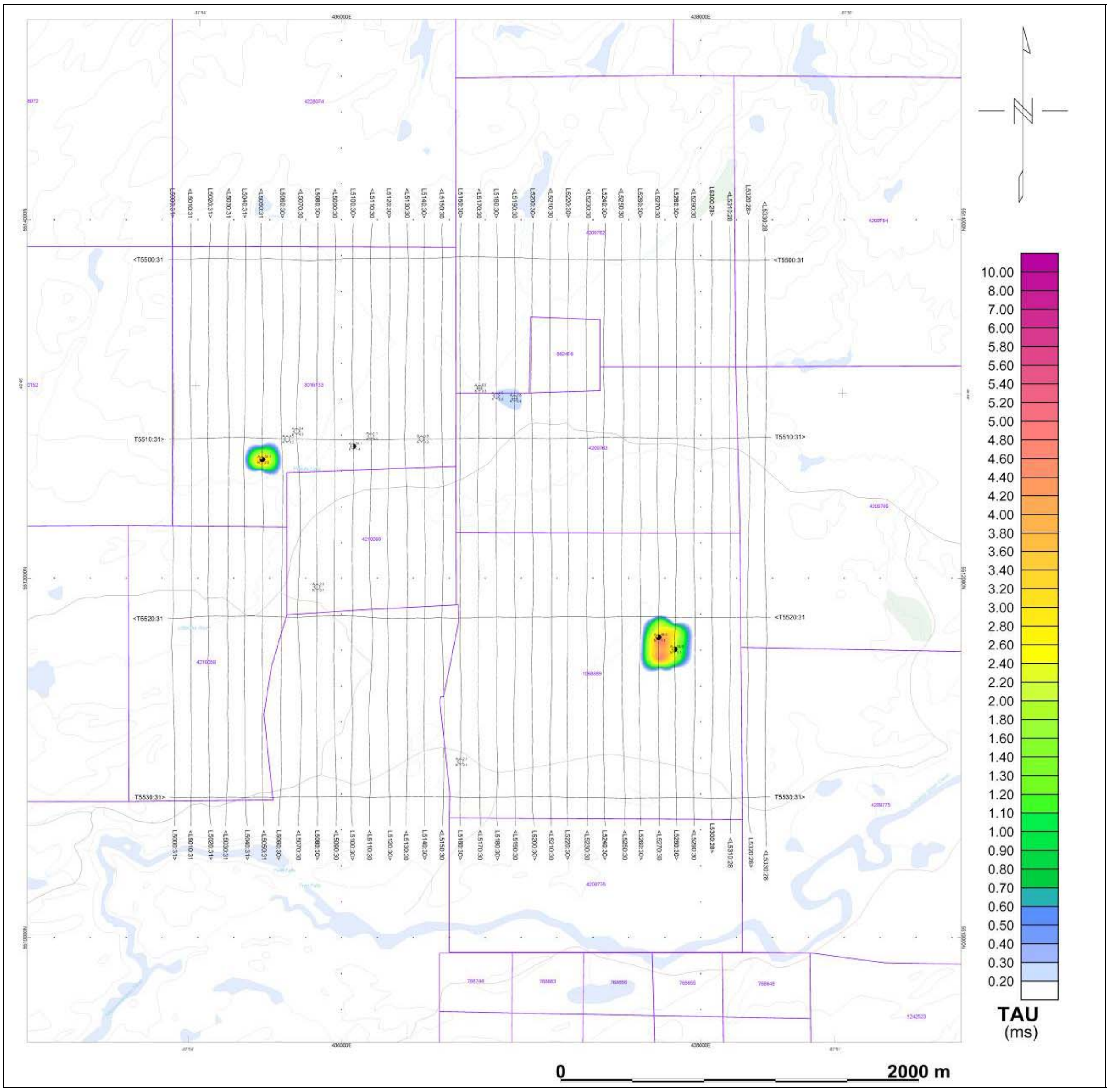

VTEM B-Field Calculated Time Constant (TAU) for the Twin Falls Block with EM anomalies

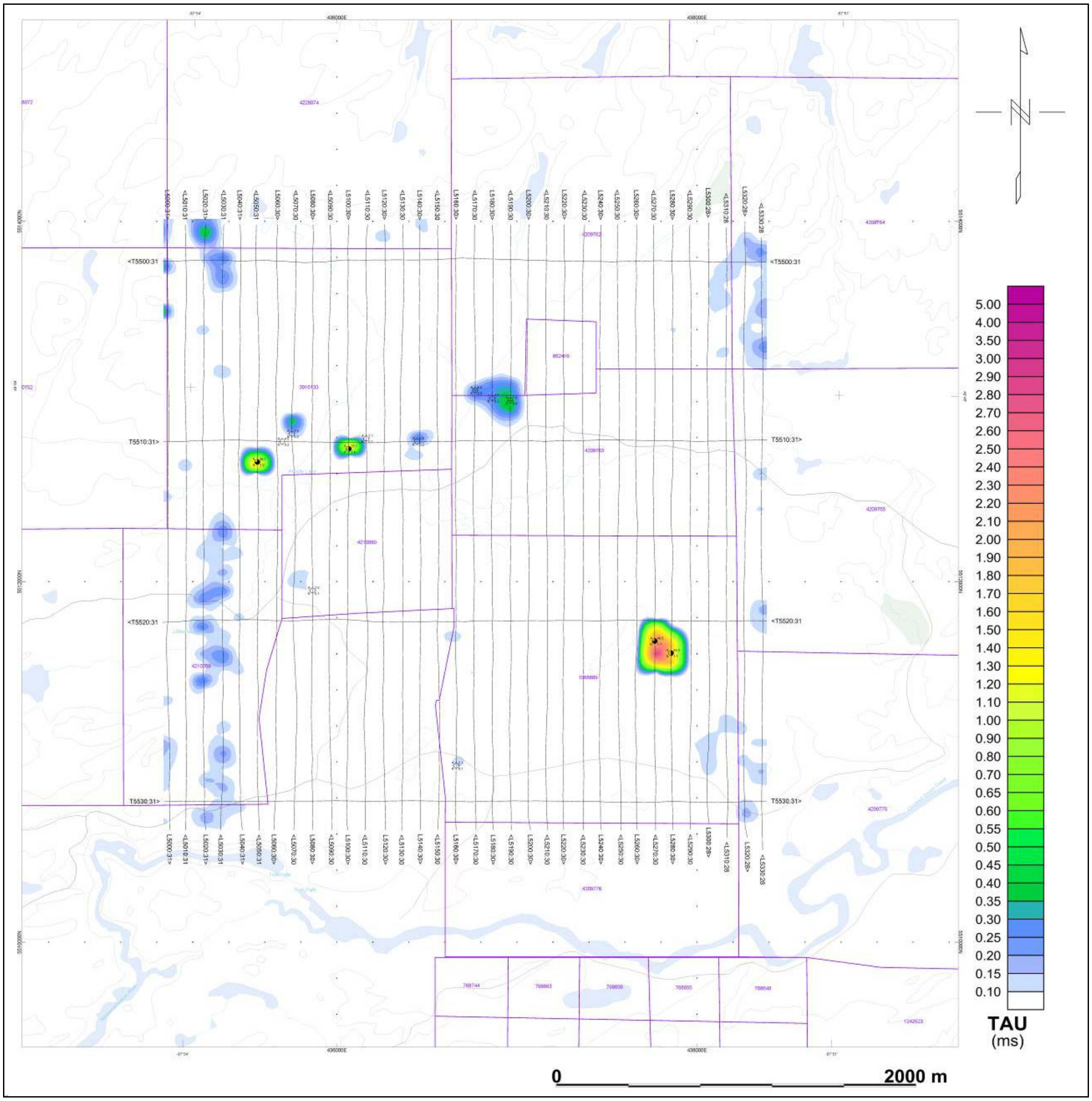

VTEM dB/dt Calculated Time Constant (TAU) for the Twin Falls Block with EM anomalies

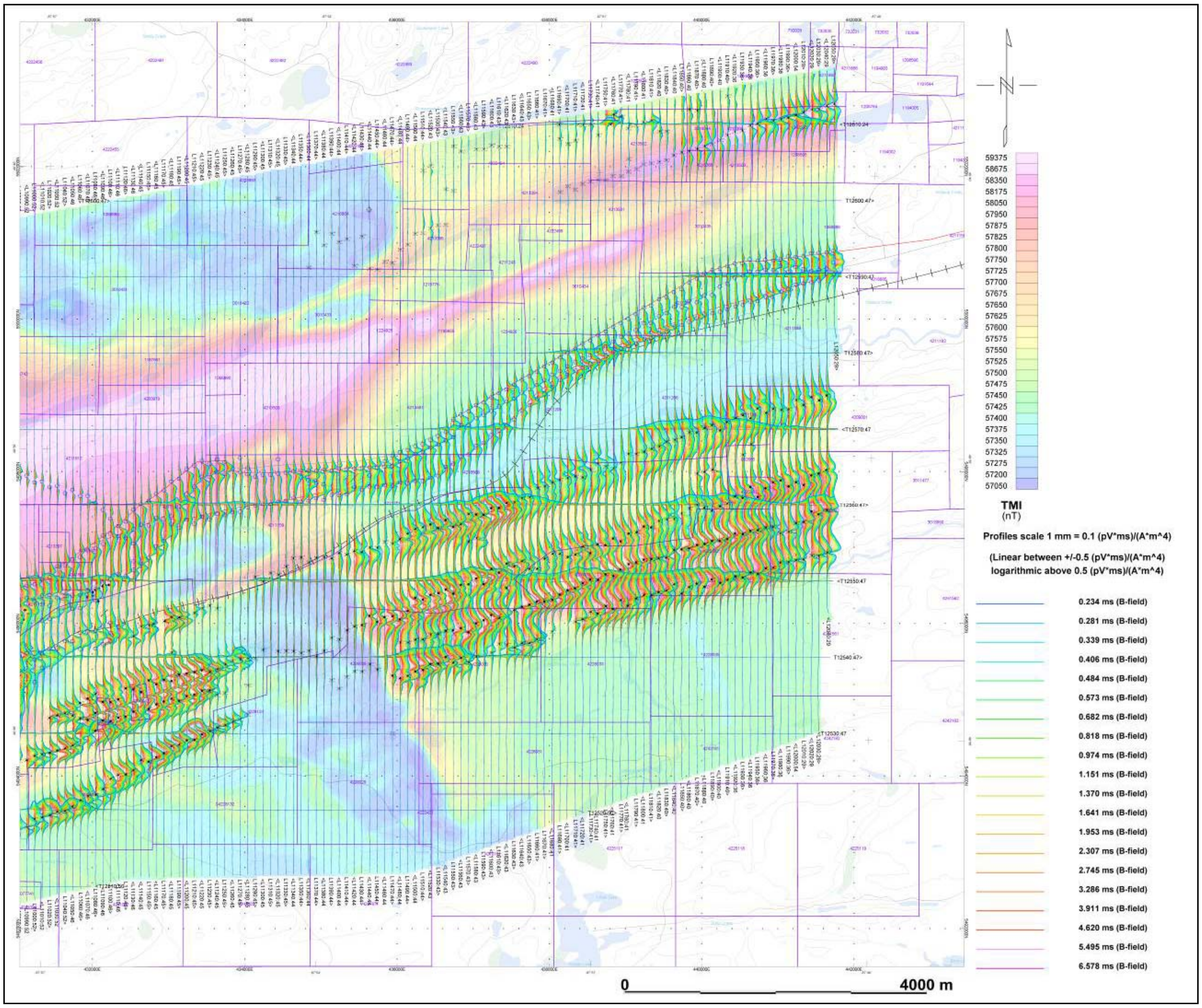

VTEM B-Field Profiles with TMI Color Image for the Empire (east) Block with EM anomalies

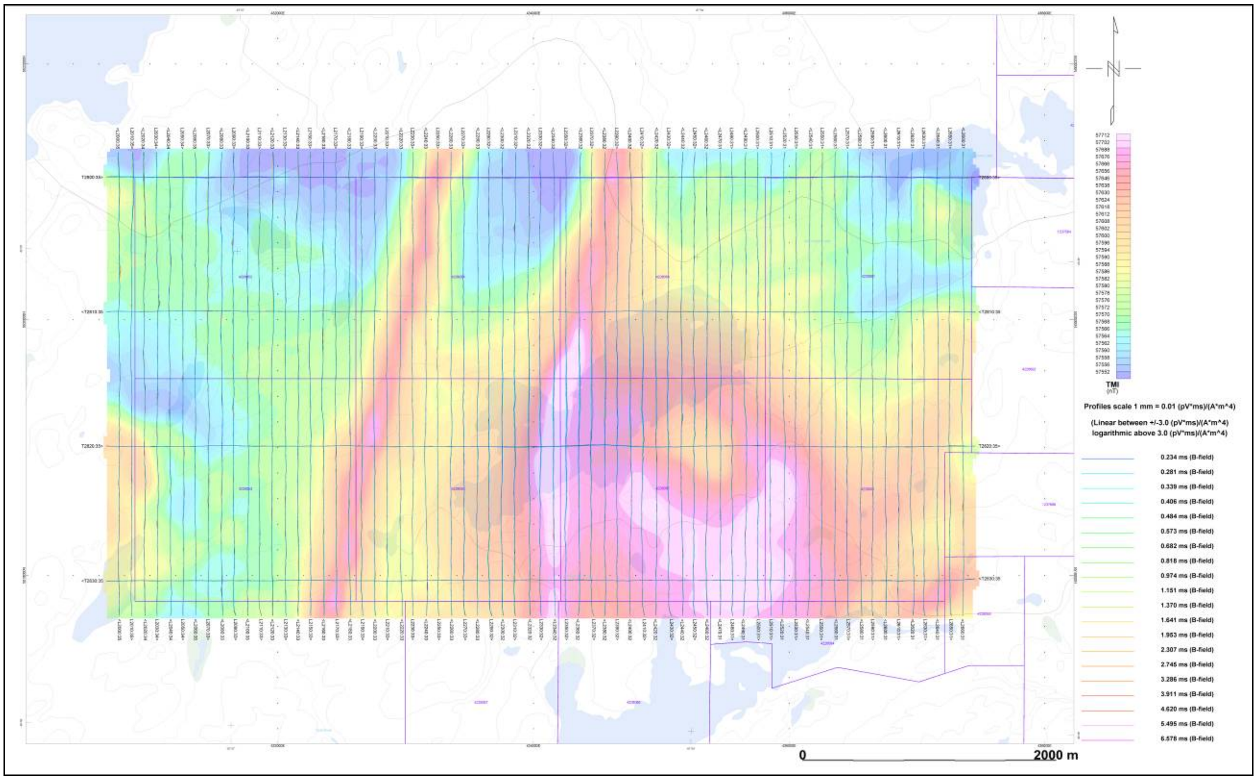

VTEM B-Field Profiles with TMI Color Image for the Forge Creek Block

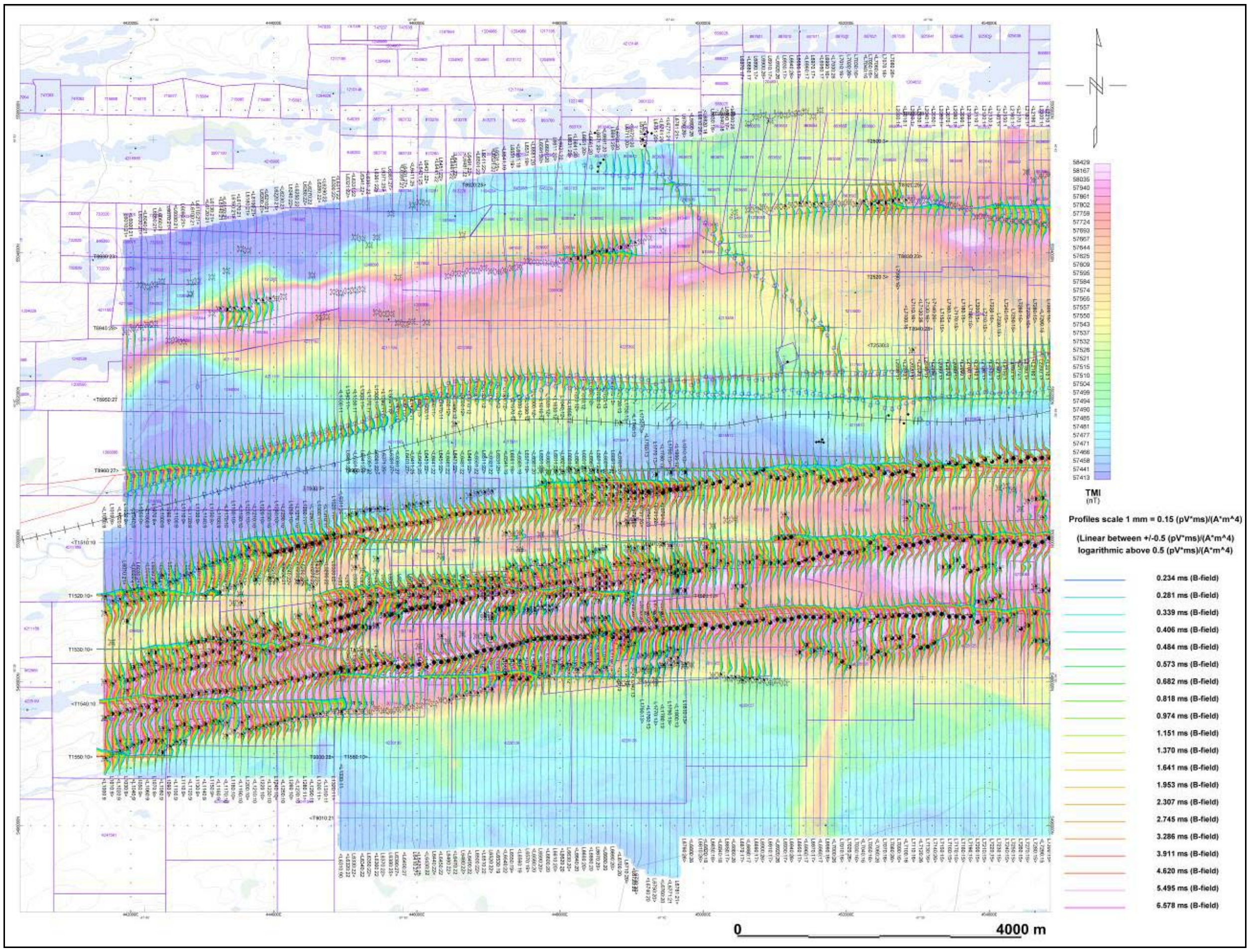

VTEM B-Field Profiles with TMI Color Image for the Lattimer (west) Block with EM anomalies

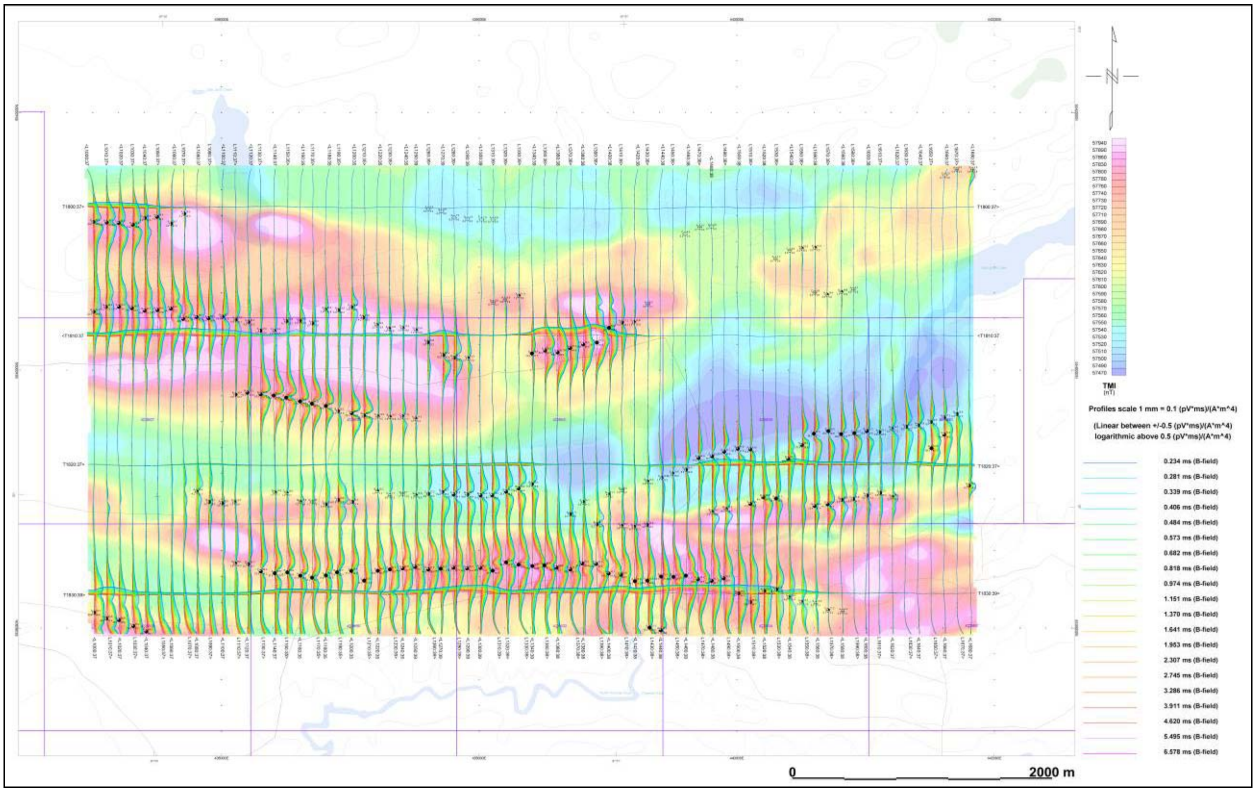

VTEM B-Field Profiles with TMI Color Image for the Little John Block with EM anomalies

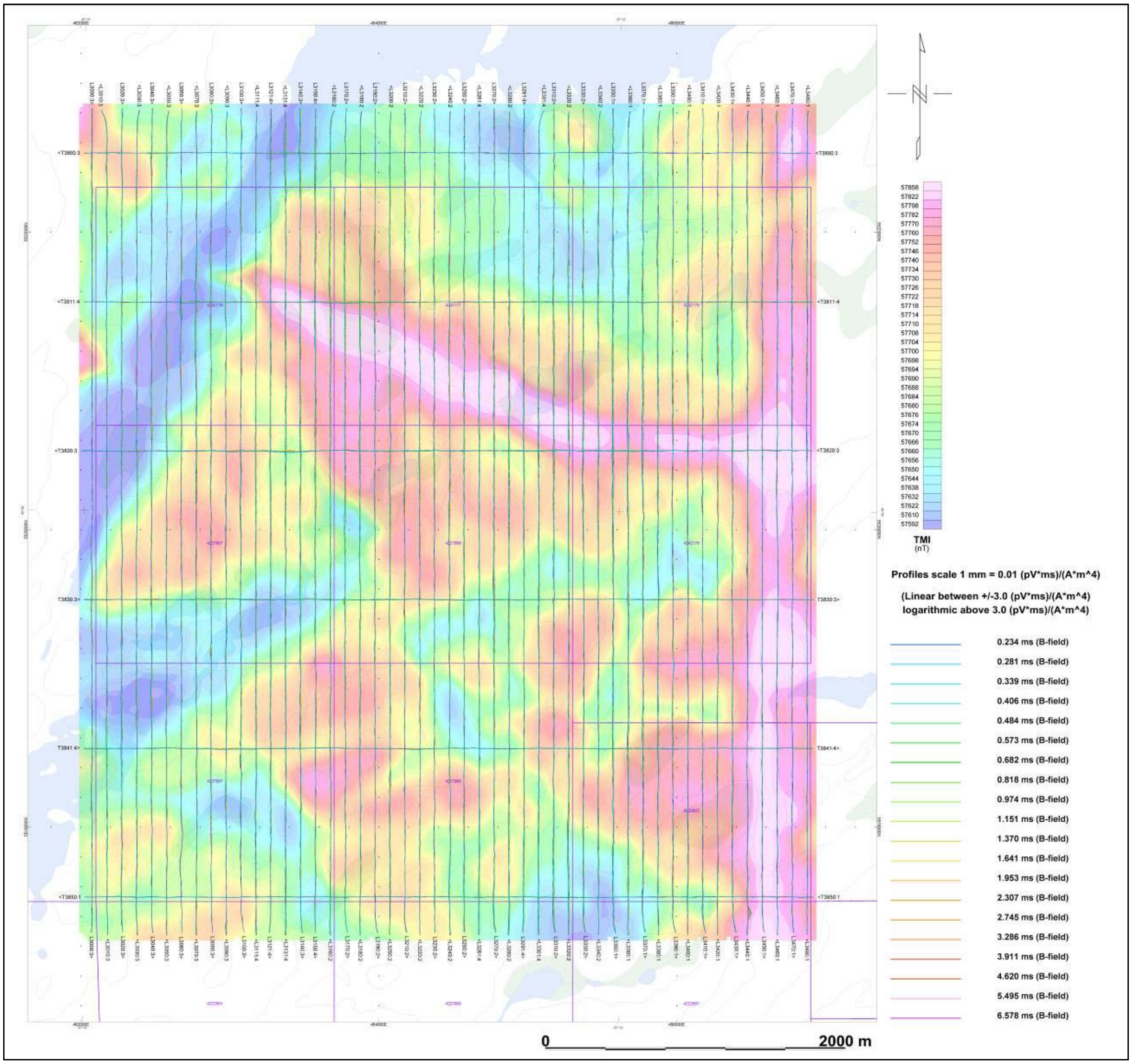

VTEM B-Field Profiles with TMI Color Image for the NIK Block

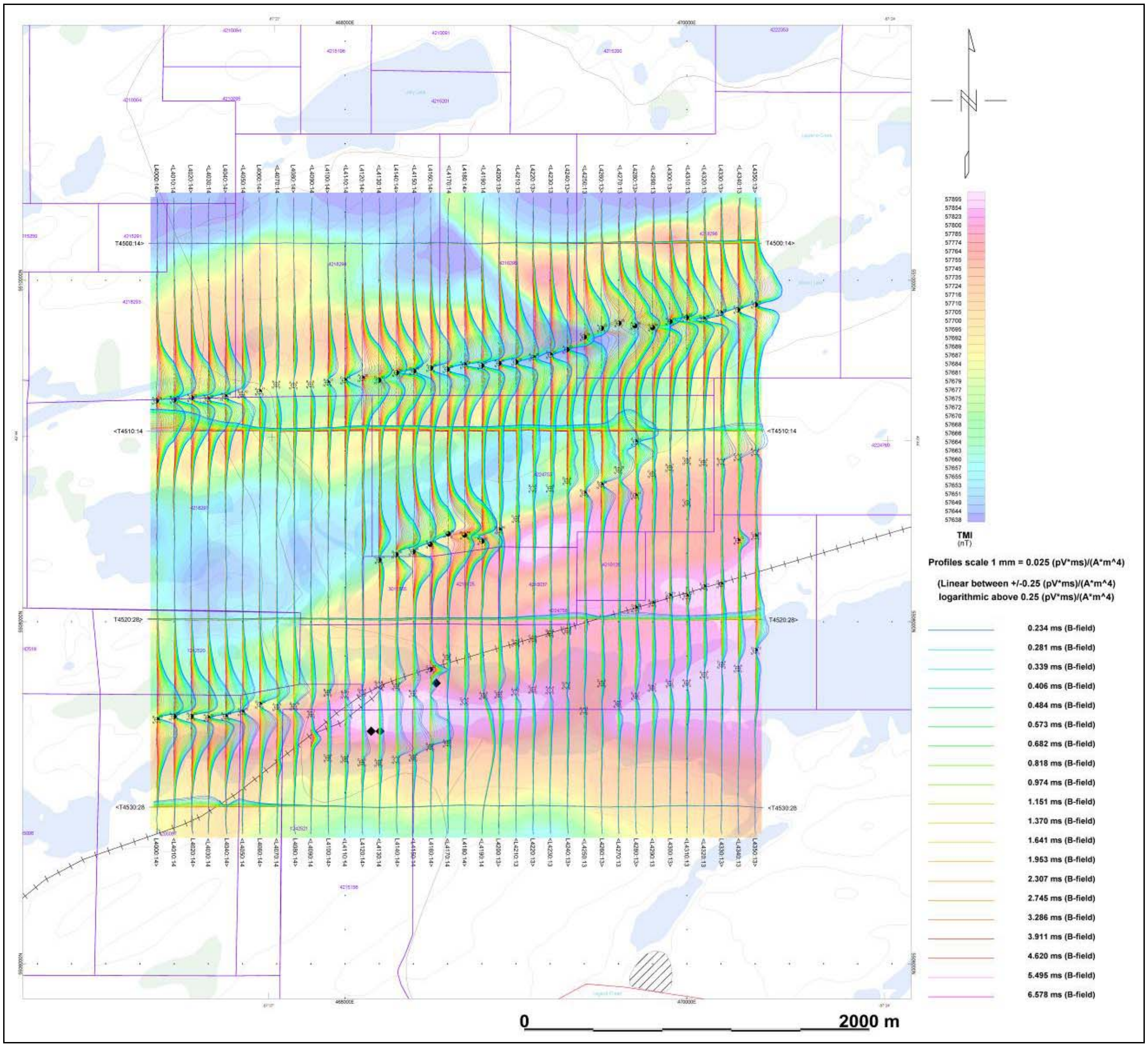

VTEM B-Field Profiles with TMI Color Image for the St. Bridge Block with EM anomalies

APPENDIX E

GENERALIZED MODELING RESULTS OF THE VTEM SYSTEM

Introduction

The VTEM system is based on a concentric or central loop design, whereby, the receiver is positioned at the centre of a 26.1 meters diameter transmitter loop that produces a dipole moment up to 625,000 nIA at peak current. The wave form is a bi-polar, modified square wave with a turn-on and turn-off at each end. With a base frequency of 30 Hz, the duration of each pulse is approximately 7.2 milliseconds followed by an off time where no primary field is present.

During turn-on and turn-off, a time varying field is produced (dB/dt) or B-field and an electro-motive force (emf) is created as a finite impulse response. A current ring around the transmitter loop moves outward and downward as time progresses. When conductive rocks and mineralization are encountered, a secondary field is created by mutual induction and measured by the receiver at the centre of the transmitter loop.

VTEM measurements are made partly during the transmitter On but primarily during the Off-time, when only the secondary fields representing the conductive targets encountered in the ground are present. The secondary fields are displayed both as dB/dt and calculated B-field responses.

Efficient modeling of the results can be carried out on regularly shaped geometries, thus yielding close approximations to the parameters of the measured targets. The following is a description of a series of common models made for the purpose of promoting a general understanding of the measured results.

General Modeling Concepts

A set of models has been produced for the Geotech VTEM® system with explanation notes (see models C1 to C18). The reader is encouraged to review these models, so as to get a general understanding of the responses as they apply to survey results. While these models do not begin to cover all possibilities, they give a general perspective on the simple and most commonly encountered anomalies.

When producing these models, a few key points were observed and are worth noting as follows:

- For near vertical and vertical plate models, the top of the conductor is always located directly under the centre low point between the two shoulders in the classic **M** shaped response.

- As the plate is positioned at an increasing depth to the top, the shoulders of the **M** shaped response, have a greater separation distance.

- When faced with choosing between a flat lying plate and a prism model to represent the target (broad response) some ambiguity is present and caution should be exercised.

- With the concentric loop system and Z-component receiver coil, virtually all types of conductors and most geometries are most always well coupled and a response is generated. Only concentric loop systems can map these varieties of target geometries.

The Maxwell ™ EM modeling program (IMIT Technologies Ltd. Pty, Midland WA, AU) used to generate the following dB/dt and B-field off-time responses all assume a conductive plate in an infinitely resistive half-spaced host rock

Variation of Plate Depth

Geometries represented by plates of different strike length, depth extent, dip, plunge and depth below surface can be varied with characteristic parameters like conductance of the target, conductance of the host and conductivity/thickness and thickness of the overburden layer.

Diagrammatic models for a vertical plate are shown in Figures C-1 & C-2 and C-5 & C-6 at two different depths, all other parameters remaining constant. With this transmitter-receiver geometry, the classic **M** shaped response is generated. Figures C-1 and C-2 show a plate where the top is near surface. Here, amplitudes of the duel peaks are higher and symmetrical with the zero centre positioned directly above the plate. Most important is the separation distance of the peaks. This distance is small when the plate is near surface and widens with a linear relationship as the plate (depth to top) increases. Figures C-5 and C-6 show a much deeper plate where the separation distance of the peaks is much wider and the amplitudes of the channels have decreased.

Variation of Plate Dip

As the plate dips and departs from the vertical position, the peaks become asymmetrical. Figures C-3 & C-4 and C-7 and C-8 show a near surface plate dipping 80º at two different depths. Note that the direction of dip is toward the high shoulder of the response and the top of the plate remains under the centre minimum.

As the dip increases, the aspect ratio (Min/Max) decreases and this aspect ratio can be used as an empirical guide to dip angles from near 90º to about 30º. The method is not sensitive enough where dips are less than about 30º. For example, for a plate dipping 45º, the minimum shoulder starts to vanish. In Figures C-9 & C-10 and C-11 & C-12, a flat lying plate is shown, relatively near surface. Note that the twin peak anomaly has been replaced by a symmetrical shape with large, bell shaped, channel amplitudes which decay relative to the conductance of the plate.

In the special case where two plates are positioned to represent a synclinal structure. Note that the main characteristic is that the centre amplitudes are higher (approximately double) compared to the high shoulder of a single plate. This model is very representative of tightly folded formations where the conductors where once flat lying.

Variation of Prism Dip

Finally, with thicker, prism models, another algorithm is required to represent current on the plate. A plate model is considered to be infinitely thin with respect to thickness and incapable of representing the current in the thickness dimension. A prism model is constructed to deal with this problem, thereby, representing the thickness of the body more accurately.

Figures C-13 & C-14 and C-15 & C-16 show the same prism at the same depths with variable dips. Aside from the expected differences asymmetry prism anomalies show a characteristic change from a double-peaked anomaly to single peak signatures.

I. THIN PLATE

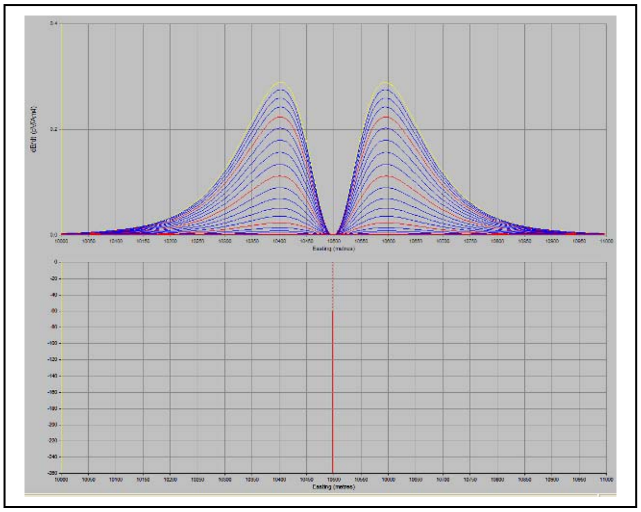

Figure C-1: dB/dt response of a shallow vertical thin plate. Depth=100 m, CT=20 S. The EM response is normalized by the dipole moment and the Rx area.

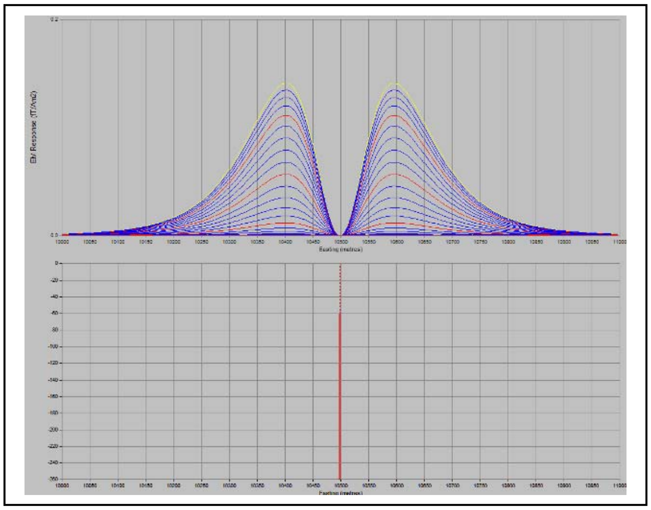

Figure C-2: B-field response of a shallow vertical thin plate. Depth=100 m, CT=20 S. The EM response is normalized by the dipole moment.

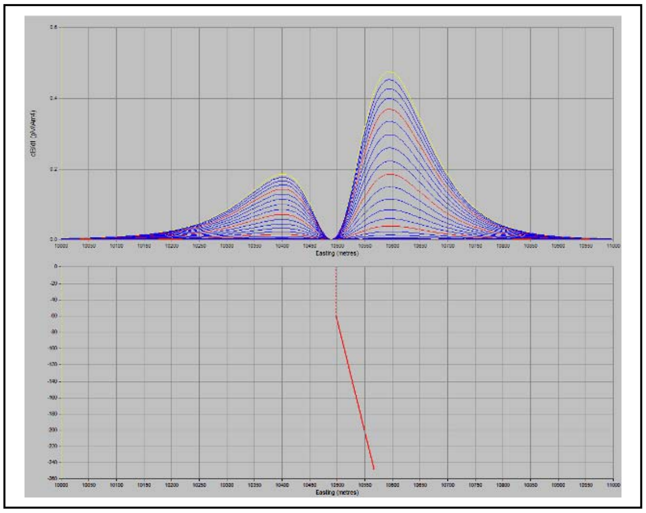

Figure C-3: dB/dt response of a shallow skewed thin plate. Depth=100 m, CT=20 S. The EM response is normalized by the dipole moment and the Rx area.

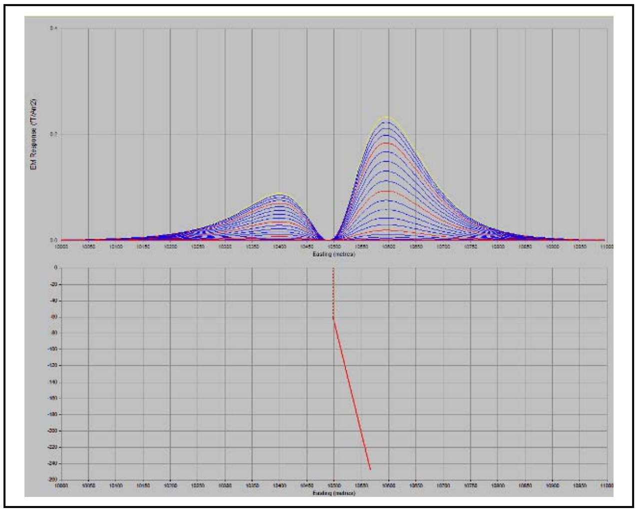

Figure C-4: B-field response of a shallow skewed thin plate. Depth=100 m, CT=20 S. The EM response is normalized by the dipole moment.

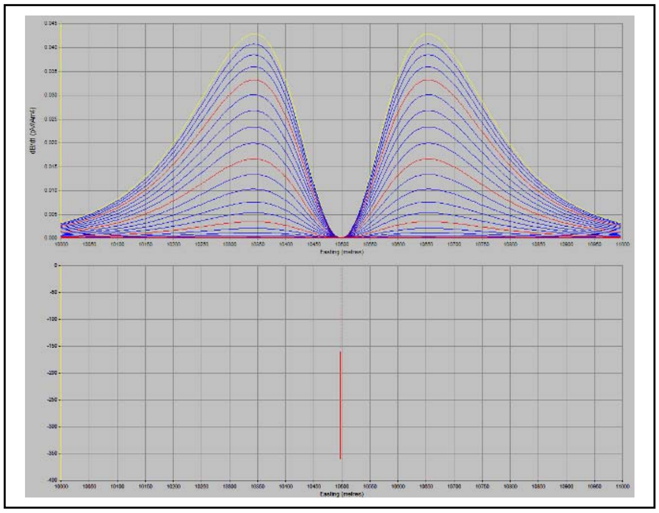

Figure C-5: dB/dt response of a deep vertical thin plate. Depth=200 m, CT=20 S. The EM response is normalized by the dipole moment and the Rx area.

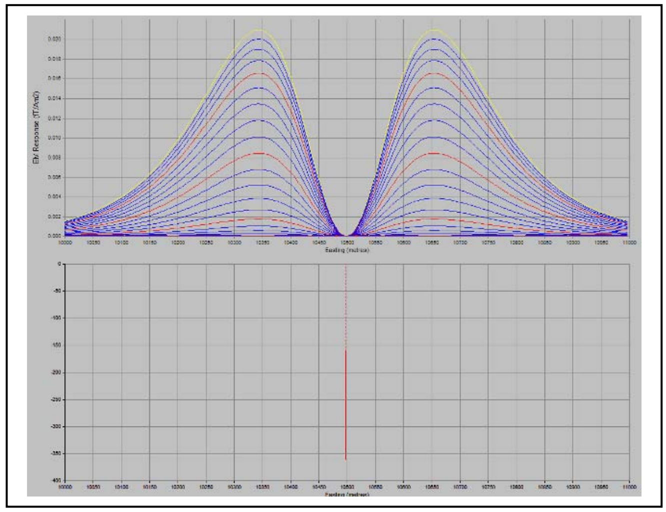

Figure C-6: B-Field response of a deep vertical thin plate. Depth=200 m, CT=20 S. The EM response is normalized by the dipole moment.

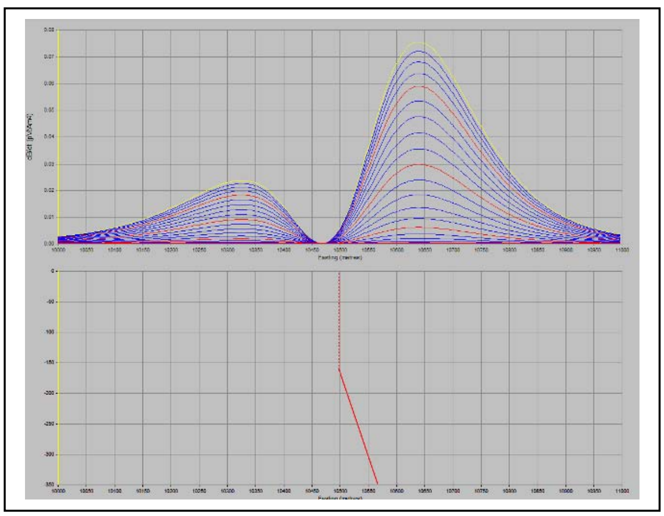

Figure C-7: dB/dt response of a deep skewed thin plate. Depth=200 m, CT=20 S. The EM response is normalized by the dipole moment and the Rx area.

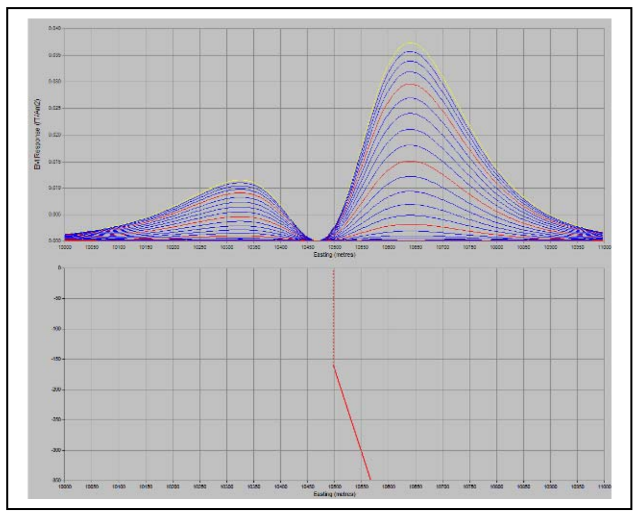

Figure C-8: B-field response of a deep skewed thin plate. Depth=200 m, CT=20 S. The EM response is normalized by the dipole moment.

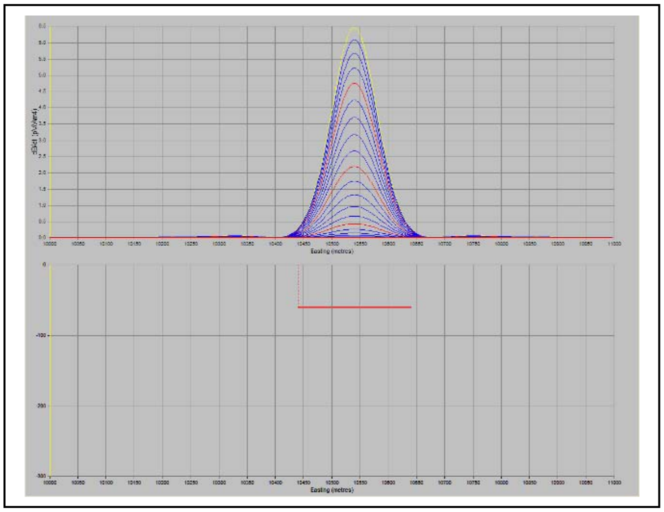

Figure C-9: dB/dt response of a shallow horizontal thin plate. Depth=100 m, CT=20 S. The EM response is normalized by the dipole moment and the Rx area.

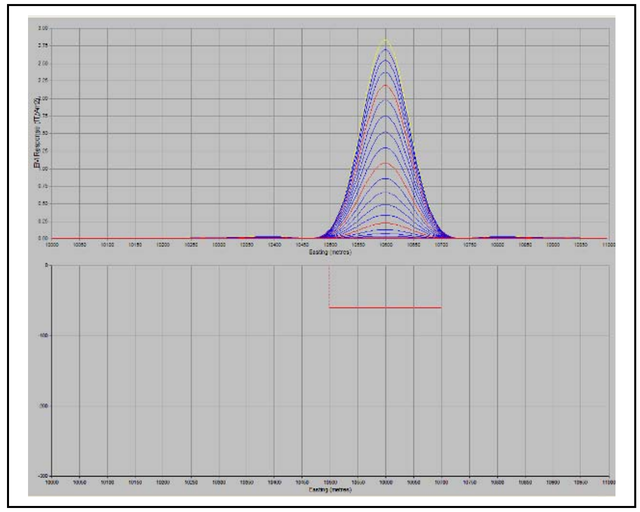

Figure C-10: B-Field response of a shallow horizontal thin plate. Depth=100 m, CT=20 S. The EM response is normalized by the dipole moment.

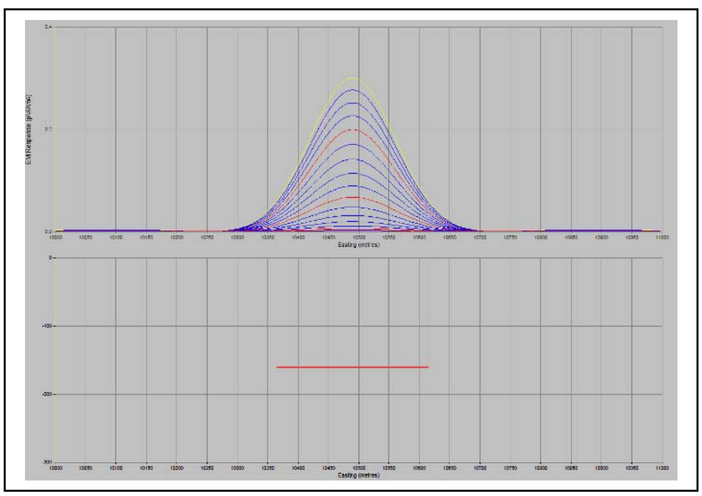

Figure C-11: dB/dt response of a deep horizontal thin plate. Depth=200 m, CT=20 S. The EM response is normalized by the dipole moment and the Rx area.

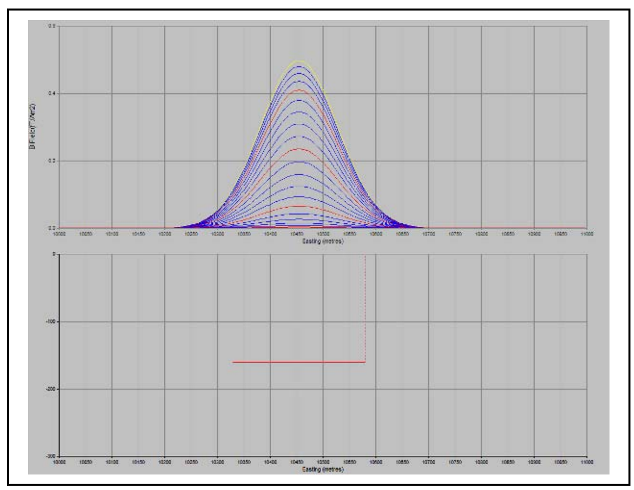

Figure C-12: B-Field response of a deep horizontal thin plate. Depth=200 m, CT=20 S. The EM response is normalized by the dipole moment.

II. THICK PLATE

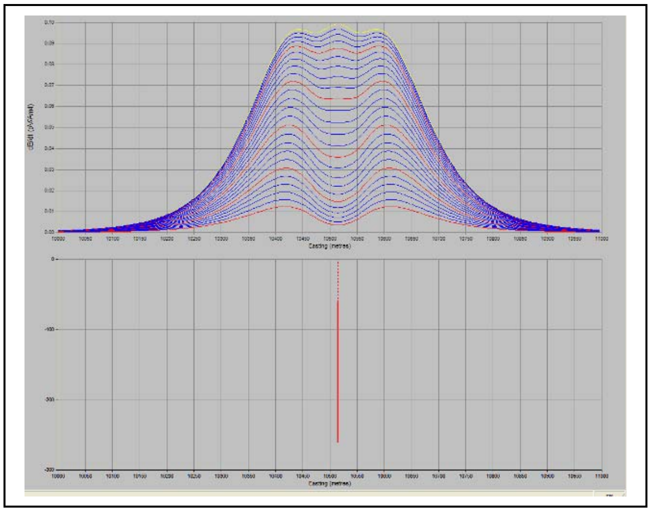

Figure C-13: dB/dt response of a shallow vertical thick plate. Depth=100 m, C=12 S/m, thickness=20 m. The EM response is normalized by the dipole moment and the Rx area.

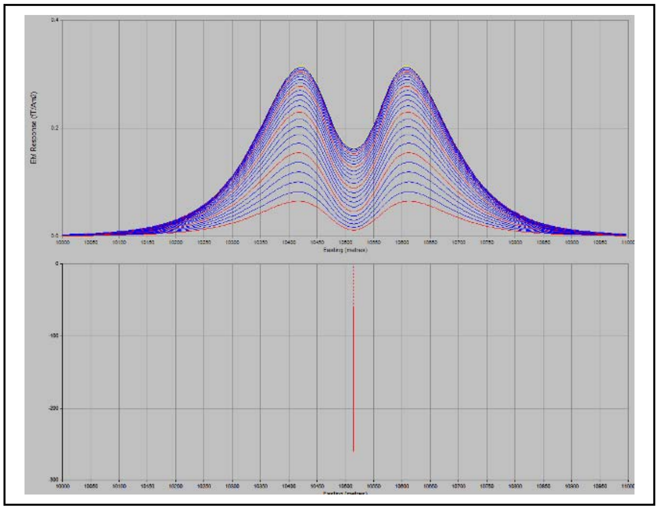

Figure C-14: B-Field response of a shallow vertical thick plate. Depth=100 m, C=12 S/m, thickness= 20 m. The EM response is normalized by the dipole moment.

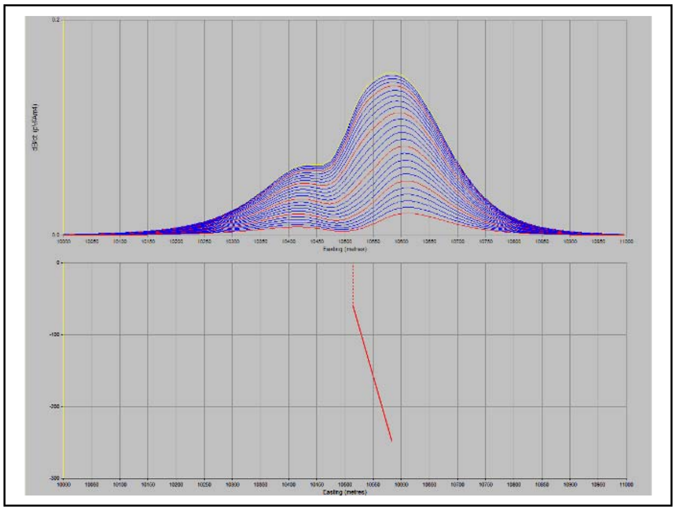

Figure C-15: dB/dt response of a shallow skewed thick plate. Depth=100 m, C=12 S/m, thickness=20 m. The EM response is normalized by the dipole moment and the Rx area.

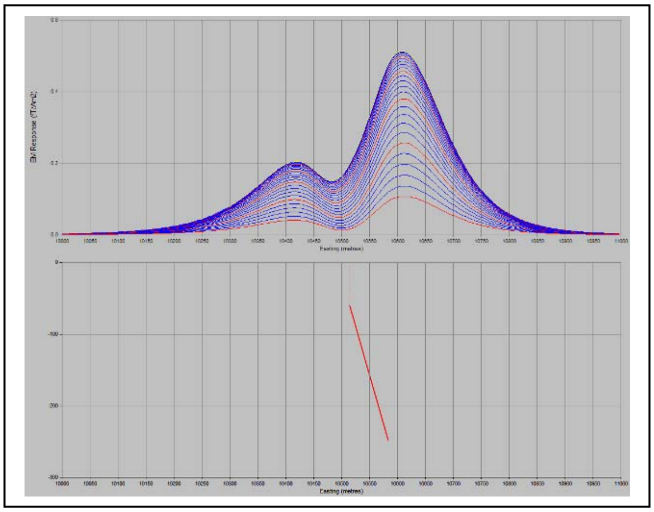

Figure C-16: B-Field response of a shallow skewed thick plate. Depth=100 m, C=12 S/m, thickness=20 m. The EM response is normalized by the dipole moment.

III. MULTIPLE THIN PLATES

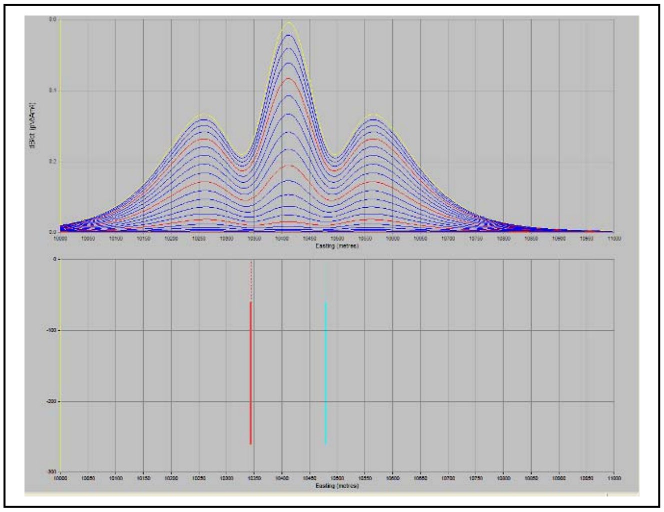

Figure C-17: dB/dt response of two vertical thin plates. Depth=100 m, CT=20 S. The EM response is normalized by the dipole moment and the Rx area.

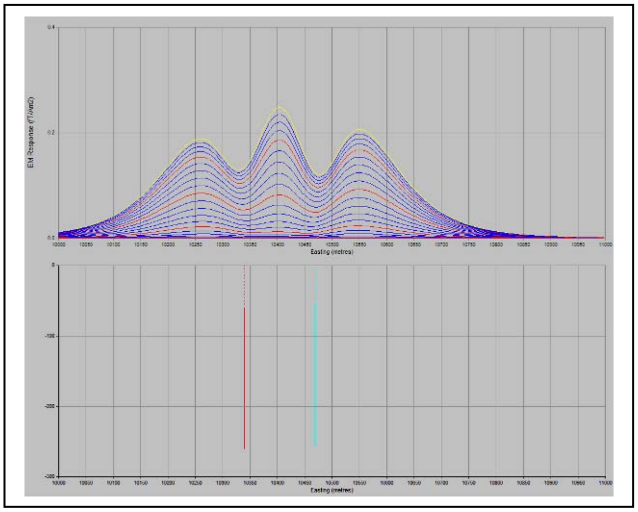

Figure C-18: B-Field response of two vertical thin plates. Depth=100 m, CT=20 S. The EM response is normalized by the dipole moment.

General Interpretation Principals

Magnetics

The total magnetic intensity responses reflect major changes in the magnetite and/or other magnetic minerals content in the underlying rocks and unconsolidated overburden. Precambrian rocks have often been subjected to intense heat and pressure during structural and metamorphic events in their history. Original signatures imprinted on these rocks at the time of formation have, it most cases, been modified, resulting in low magnetic susceptibility values.

The amplitude of magnetic anomalies, relative to the regional background, helps to assist in identifying specific magnetic and non-magnetic rock units (and conductors) related to, for example, mafic flows, mafic to ultramafic intrusives, felsic intrusives, felsic volcanics and/or sediments etc. Obviously, several geological sources can produce the same magnetic response. These ambiguities can be reduced considerably if basic geological information on the area is available to the geophysical interpreter.

In addition to simple amplitude variations, the shape of the response expressed in the wave length and the symmetry or asymmetry, is used to estimate the depth, geometric parameters and magnetization of the anomaly. For example, long narrow magnetic linears usually reflect mafic flows or intrusive dyke features. Large areas with complex magnetic patterns may be produced by intrusive bodies with significant magnetization, flat lying magnetic sills or sedimentary iron formation. Local isolated circular magnetic patterns often represent plug-like igneous intrusives such as kimberlites, pegmatites or volcanic vent areas.

Because the total magnetic intensity (TMI) responses may represent two or more closely spaced bodies within a response, the second derivative of the TMI response may be helpful for distinguishing these complexities. The second derivative is most useful in mapping near surface linears and other subtle magnetic structures that are partially masked by nearby higher amplitude magnetic features. The broad zones of higher magnetic amplitude, however, are severely attenuated in the vertical derivative results. These higher amplitude zones reflect rock units having strong magnetic susceptibility signatures. For this reason, both the TMI and the second derivative maps should be evaluated together.

Theoretically, the second derivative, zero contour or color delineates the contacts or limits of large sources with near vertical dip and shallow depth to the top. The vertical gradient map also aids in determining contact zones between rocks with a susceptibility contrast, however, different, more complicated rules of thumb apply.

Concentric Loop EM Systems

Concentric systems with horizontal transmitter and receiver antennae produce much larger responses for flat lying conductors as contrasted with vertical plate-like conductors. The amount of current developing on the flat upper surface of targets having a substantial area in this dimension, are the direct result of the effective coupling angle, between the primary magnetic field and the flat surface area. One therefore, must not compare the amplitude/conductance of responses generated from flat lying bodies with those derived from near vertical plates; their ratios will be quite different for similar conductances.

Determining dip angle is very accurate for plates with dip angles greater than 30º. For angles less than 30º to 0º, the sensitivity is low and dips can not be distinguished accurately in the presence of normal survey noise levels.

A plate like body that has near vertical position will display a two shoulder, classic **M** shaped response with a distinctive separation distance between peaks for a given depth to top.

It is sometimes difficult to distinguish between responses associated with the edge effects of flat lying conductors and poorly conductive bedrock conductors. Poorly conductive bedrock conductors having low dip angles will also exhibit responses that may be interpreted as surfacial overburden conductors. In some situations, the conductive response has line to line continuity and some magnetic correlation providing possible evidence that the response is related to an actual bedrock source.

The EM interpretation process used, places considerable emphasis on determining an understanding of the general conductive patterns in the area of interest. Each area has different characteristics and these can effectively guide the detailed process used.

The first stage is to determine which time gates are most descriptive of the overall conductance patterns. Maps of the time gates that represent the range of responses can be very informative.

Next, stacking the relevant channels as profiles on the flight path together with the second vertical derivative of the TMI is very helpful in revealing correlations between the EM and Magnetics.

Next, key lines can be profiled as single lines to emphasize specific characteristics of a conductor or the relationship of one conductor to another on the same line. Resistivity Depth sections can be constructed to show the relationship of conductive overburden or conductive bedrock with the conductive anomaly.

____

Roger Barlow
Consultant

____

Nasreddine Bournas, P. Geo.
Geophysicist
Geotech Ltd.

December 2008

APPENDIX F

EM TIME CONSTANT (TAU) ANALYSIS

Theory

As established in electromagnetic theory, the magnitude of the electro-motive force (emf) induced is proportional to the time rate of change of primary magnetic field at the conductor. This emf causes eddy currents to flow in the conductor with a characteristic decay, whose Time Constant (Tau) is a function of the conductivity and geometry of the survey target. The decaying currents generate a proportional secondary magnetic field, the time rate of change of which is measured by the receiver coil as induced voltage during the Off time.

The receiver coil output voltage (**e_0**) is proportional to the time rate of change of the secondary magnetic field and has the form,

$$e_0 \; \alpha \; (1 / \tau) \; e^{-(t/\tau)}$$

Where,
τ = L/R is the characteristic time constant of the target
R = resistance
L = inductance

From the expression, conductive targets that have small value of resistance and hence large value of τ yield signals with small initial amplitude that decays relatively slowly with progress of time. Conversely, signals from poorly conducting targets that have large resistance value and small τ, have high initial amplitude but decay rapidly with time[11].

EM Time Constant (Tau) Calculation

The EM Time-Constant (TAU) is a general measure of the speed of decay of the electromagnetic response and indicates the presence of eddy currents in conductive sources as well as reflecting the "conductance quality" of a source. Although Tau can be calculated using either the measured dB/dt decay or the calculated B-field decay, dB/dt is commonly preferred due to better stability (S/N) relating to signal noise. Generally, TAU calculated on base of early time response reflects both near surface overburden and poor conductors whereas, in the late ranges of time, deep and more conductive sources, respectively. For example early time TAU distributions in an area that is indicate of conductive overburden are shown in Figure 1.

11 McNeill, JD, 1980, "Applications of Transient Electromagnetic Techniques", Technical Note TN-7 page 5 Geonics Limited, Mississauga, Ontario.

1 McNeill, JD, 1980, “Applications of Transient Electromagnetic Techniques”, Technical Note TN-7 page 5, Geonics Limited, Mississauga, Ontario.

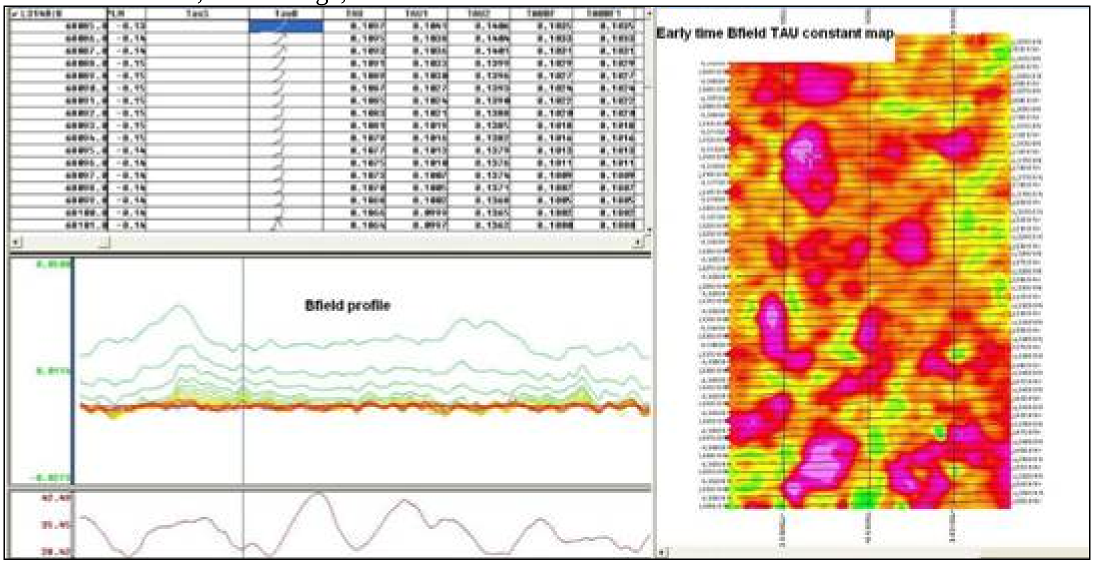

Figure F1 - Area with overburden conductive layer and local sources.

If TAU is calculated across a wide range of time it becomes an integrated parameter and can be used to differentiate conductive sources (Figure 2).

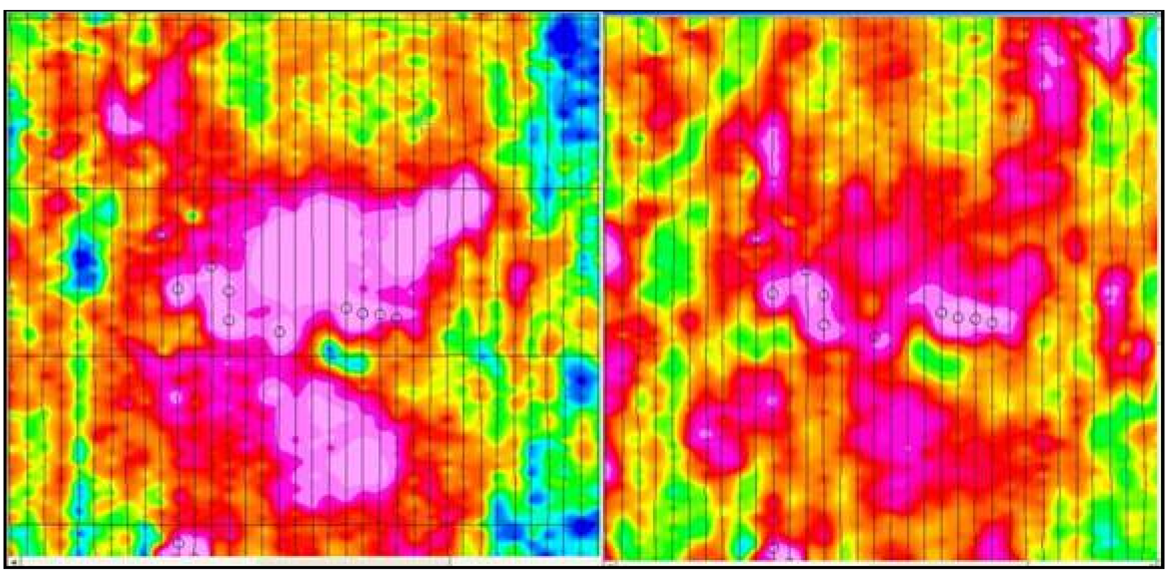

Figure F2 - Map of B-field (left) and TAU (right) with EM anomaly picks due to deep conductive targets.

There are many advantages of TAU maps:

- Because TAU is time integral parameter, all conductive zones and targets are displayed independently of their depth and conductivity on a single map.

- Very good differential resolution in complex conductive places with many sources with different conductivity.
- Signs of the presence of good conductive targets are amplified and emphasized independently of their depth and level of response accordingly.
- Targets which create negative responses in certain known geologic situations, for example due to the relative location of the target, the conductive cover and the coincident geometry of the VTEM system, will usually produce a positive TAU.

In the example shown in Figure 3, three local targets are defined, each of them with a different depth of burial, as indicated on the conductivity depth image (CDI). All are very good conductors but the deeper target (number 3) has a relatively weak dB/dt signal yet also features the strongest total TAU (Figure 4). This example highlights the benefit of Tau analysis in terms of an additional target discrimination tool.

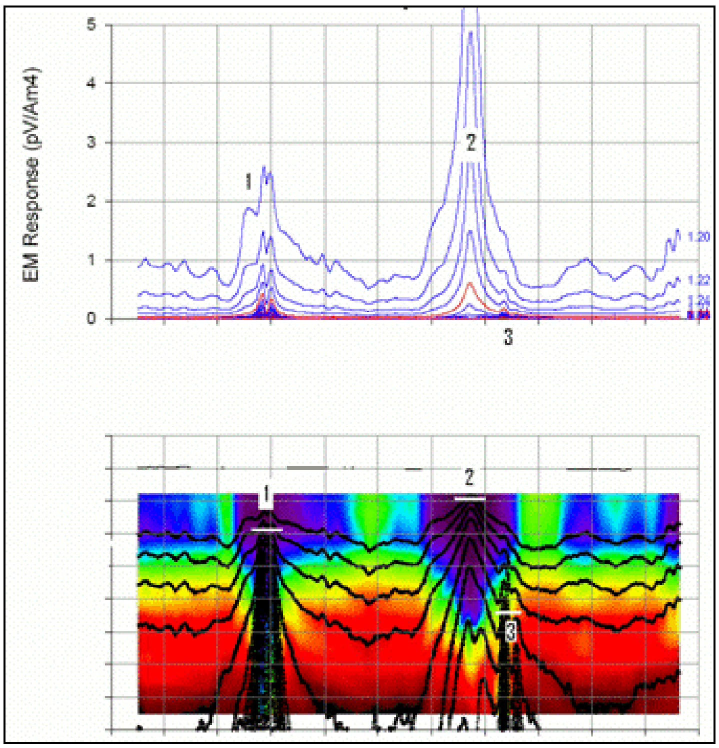

Figure F3 – dB/dt profile and CDI with different depths of sources (white lines).

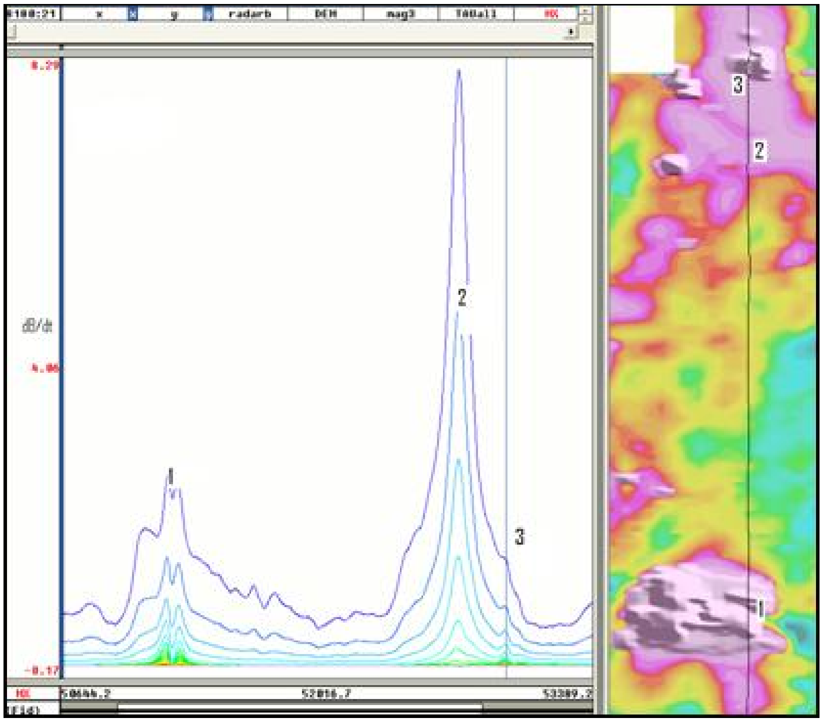

Figure F4 – Map of total TAU and dB/dt profile.

The dB/dt and B decays are measured over 24 gates named SF_10 to SF_33 (dB/dt) and BF_10 to BF_33 (B-Field). Time constants are taken from a least squares fit of a straight line (log/linear space) over the last 4 gates above a noise threshold. Threshold settings are 0.01pV/Am4 (dB.dt) and 0.015 pVmsec/Am4 (B-field). As amplitude increases, the time constant is taken at later times of the decay. As amplitudes decreases, the time constant is taken at early times of the decay. If amplitudes are very low and there is not 4 gates above the threshold, the time constant is set to zero.

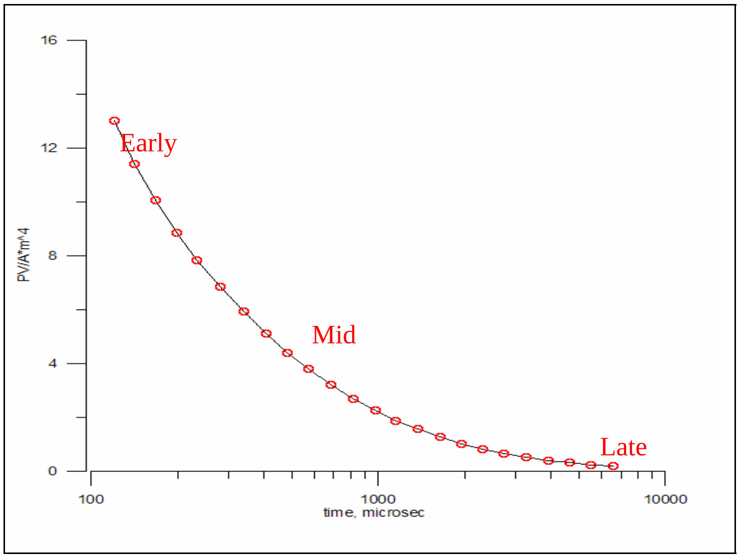

Figure F5 - Typical dB/dt decays of Vtem data

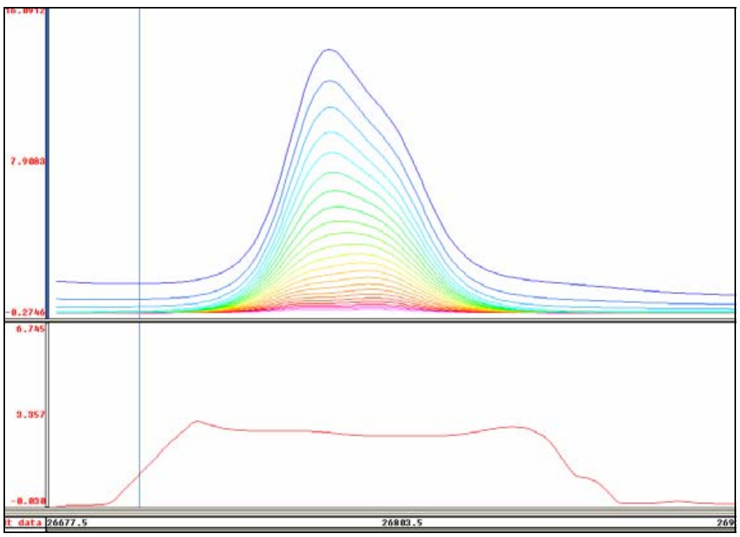

Figure F6 - Vtem anomaly and EM Time constant graph.

Alexander Prikhodko, PhD
Geotech Ltd.

Nasreddine Bournas, PhD, P. Geo (QC)
Geotech Ltd.

December 2008

APPENDIX G

ELECTROMAGNETIC ANOMALY LISTING

For Appendix G please see excel spreadsheets on the provided DVD